22巻　第12号　33−38　2006

田口文広：重症急性呼吸器症候群（SARS）　分子呼吸器病　第11巻　第1号　42−47　2007

田口文広：SARS コロナウイルス感染症　臨床とウイルス　第43巻　第5号　423-428 2006

石井孝司、水谷哲也　SARS コロナウイルス研究の最前線　医学のあゆみ　218：839-844 2006

International Immunology Advance Access published August 16, 2004

International Immunology 2004; 1 of 8
doi:10.1093/intimm/dxh143

© 2004 The Japanese Society for Immunology

A subcutaneously injected UV-inactivated SARS coronavirus vaccine elicits systemic humoral immunity in mice

Naomi Takasuka[1], Hideki Fujii[1], Yoshimasa Takahashi[1], Masataka Kasai[1], Shigeru Morikawa[2], Shigeyuki Itamura[4], Koji Ishii[3], Masahiro Sakaguchi[1], Kazuo Ohnishi[1], Masamichi Ohshima[1], Shu-ichi Hashimoto[1], Takato Odagiri[4], Masato Tashiro[4], Hiroshi Yoshikura[5], Toshitada Takemori[1] and **Yasuko Tsunetsugu-Yokota[1]**

[1]Department of Immunology, [2]First, [3]Second and [4]Third Departments of Virology, [5]National Institute of Infectious Diseases, Toyama 1-23-1, Shinjuku-ku, Tokyo 162-8640, Japan

Keywords: alum, cellular immunity, neutralizing antibody, parenteral administration, vaccination

Abstract

The recent emergence of severe acute respiratory syndrome (SARS) was caused by a novel coronavirus, SARS-CoV. It spread rapidly to many countries and developing a SARS vaccine is now urgently required. In order to study the immunogenicity of UV-inactivated purified SARS-CoV virion as a vaccine candidate, we subcutaneously immunized mice with UV-inactivated SARS-CoV with or without an adjuvant. We chose aluminum hydroxide gel (alum) as an adjuvant, because of its long safety history for human use. We observed that the UV-inactivated SARS-CoV virion elicited a high level of humoral immunity, resulting in the generation of long-term antibody secreting and memory B cells. With the addition of alum to the vaccine formula, serum IgG production was augmented and reached a level similar to that found in hyper-immunized mice, though it was still insufficient to elicit serum IgA antibodies. Notably, the SARS-CoV virion itself was able to induce long-term antibody production even without an adjuvant. Anti-SARS-CoV antibodies elicited in mice recognized both the spike and nucleocapsid proteins of the virus and were able to neutralize the virus. Furthermore, the UV-inactivated virion induced regional lymph node T-cell proliferation and significant levels of cytokine production (IL-2, IL-4, IL-5, IFN-γ and TNF-α) upon restimulation with inactivated SARS-CoV virion *in vitro*. Thus, a whole killed virion could serve as a candidate antigen for a SARS vaccine to elicit both humoral and cellular immunity.

Introduction

A new disease called severe acute respiratory syndrome (SARS) originated in China in late 2002 and spread rapidly to many countries. Upon this outbreak, a global collaboration network was coordinated by WHO. As a result of this unprecedented international effort, a novel type of coronavirus (SARS-CoV) was identified as the etiologic agent of SARS (1,2) in March 2003. The genomic sequence of SARS-CoV was completed and we now know that SARS-CoV has all the features and characteristics of other coronaviruses, but it is quite different from all previously known coronaviruses (groups I~III), representing a new group (group IV) (3,4). It is assumed that SARS-CoV is a mutant coronavirus transmitted from a wild animal that developed the ability to productively infect humans (3,5). The genome of SARS-CoV is a single-stranded plus-sense RNA ~30 kb in length and containing five major open reading frames that encode non-structural replicase polyproteins and structural proteins: the spike (S), envelope (E), membrane (M) and nucleocapsid protein (N), in the same order and of approximately the same sizes as those of other coronaviruses (5).

The reason why SARS-CoV induces severe respiratory distress in some, but not all, infected individuals is still unclear. In patients with SARS and probable SARS cases, virus is detected in sputum, stool and plasma by RT-PCR (1,2). These patients developed serum antibodies against SARS-CoV and high antibody titers against N protein were maintained for more than 5 months after infection (6). Because of their generally poor pathogenicity and difficulty of propagation

Correspondence to: Y. Tsunetsugu-Yokota; E-mail: yyokota@nih.go.jp

Transmitting editor: K. Sugamura

Received 6 May 2004, *accepted* 15 July 2004

in vitro, there have been few studies regarding immunity to human coronaviruses OC43 and 229E. In the veterinary field, however, coronaviruses have been known for many years to cause a variety of lung, liver and gut diseases in animals. As we learned from these animal models, both humoral and cellular immune responses may contribute to protection against coronavirus diseases, including SARS [for review see (7)].

The clinical manifestation of SARS is hardly distinct from other common respiratory viral infections including influenza. Because an influenza epidemic may occur simultaneously with the re-emergence of SARS, it is urgently required that we develop effective SARS vaccines as well as sensitive diagnostic tests specific for SARS. Recently, the angiotensin-converting enzyme 2 (ACE2) was identified as a cellular receptor for SARS-CoV (8). The first step in viral infection is presumably the binding of S protein to its receptor, ACE2. In the murine MHV model, S proteins are known to contain important virus-neutralizing epitopes that elicit neutralizing antibodies in mice (9,10). Therefore, the S protein would be the first candidate coronavirus protein for induction of immunity. However, the S, M and N proteins are also known to contribute to generating the host immune response (11,12).

Following an established vaccine protocol is one of the best ways to shorten the time and cost of new vaccine development. Most of the currently available vaccines for humans are inactivated and applied cutaneously, except oral polio vaccine, and adjuvant usage is mostly limited to aluminum hydroxide gel (alum). In order to know the immunogenicity of inactivated SARS-CoV as a vaccine candidate, we immunized mice with UV-inactivated SARS-CoV either with or without alum. We report here the evaluation of humoral and cellular immunity elicited by UV-inactivated SARS-CoV administered subcutaneously.

Methods

Preparation of UV-inactivated purified SARS-CoV

SARS-CoV (HKU39849) was kindly supplied by Dr J.S.M. Peiris, Department of Microbiology, The University of Hong Kong. The virus was amplified in Vero E6 cells and purified by sucrose density gradient centrifugation. Concentrated virus was then exposed to UV light (4.75 J/cm^2) in order to inactivate the virus. We confirmed that the virus completely lost its infectivity by this method.

Immunization of mice

Female BALB/c mice were purchased from Nippon SLC Inc. (Shizuoka, Japan) and were housed under specific pathogen-free conditions. All experimental procedures were carried out under NIID-recommended guidelines. Mice were subcutaneously injected via their back or right and left hind leg footpads with 10 μg of UV-inactivated purified SARS-CoV with or without 2 mg of alum, and boosted by the same procedure 7 weeks after priming.

Detection of immunoglobulins in the serum samples

Blood was obtained from the tail vein and allowed to clot overnight at 4°C. Sera were then collected by centrifugation. For ELISA, microtiter plates (Dynatech, Chantily, VA) were coated overnight at 4°C with SARS-CoV-infected or mock-infected Vero E6 cell lysates, which had been treated with 1% NP40 followed by UV-inactivation. To detect S or N protein, the plates were coated with 1% NP40 lysates of chick embryo fibroblasts that had been infected with S or N protein-expressing DIs (attenuated vaccinia virus) (13). The plates were blocked with 1% OVA in PBS–Tween (0.05%) and then incubated with the sera serially diluted at 1:25–1:10^5 for 1 h at room temperature. Plates were incubated with either peroxidase-conjugated anti-mouse IgG (1:2000, Zymed, San Francisco, CA), IgM or IgA (1:2000, Southern Biotechnology, Birmingham, AL) antibody. For detection of IgG subclasses, either peroxidase-conjugated anti-mouse IgG_1, IgG_{2a}, IgG_{2b} (1:2000, Zymed) or IgG_3 (1:2000, Southern Biotechnology) was used. Plates were washed three times with PBS–Tween at each step. Antibodies were detected by *O*-phenylenediamine (Zymed), and the absorbance of each well was read at 490 nm using a model 680 microplate reader (Bio-Rad, Hercules, CA). As a standard for IgG detection, serum was obtained from a hyper-immunized mouse; the OD490nm value of 100 U/ml standard was ~3 in all assays. SARS-CoV-specific IgG titer was calculated as follows: SARS-specific IgG titer (U/ml) = (the unit value obtained at wells coated with virus-infected cell lysates) – (the unit value obtained at wells coated with non-infected cell lysates).

ELISPOT assay for antibody-secreting cells (ASCs)

Recombinant N protein (amino acids 1–49 and 340–390) of SARS-CoV (Biodesign, Saco, ME) was diluted to 10 μg/ml in PBS, and then added at 100 μl per well to plates supported by a nitrocellulose filter (Millipore, Bedford, MA). After overnight incubation at 4°C, the plates were washed with PBS three times and then blocked at 4°C overnight with 1% OVA in PBS–Tween (0.05%). After erythrocyte lysis, single cell suspensions from BMs were suspended in RPMI supplemented with 10% FCS, 5 × 10^{-5} M 2ME, 2 mM L-glutamine, 100 U/ml penicillin and 100 μg/ml streptomycin, and then applied to the plates at a concentration of 3 × 10^5 cells per well. After 24 h cultivation, the plates were recovered and stained with alkaline phosphatase-conjugated anti-mouse IgG_1 antibody (Southern Biotechnologies). Alkaline phosphatase activity was visualized using 3-amino-ethyl carbozole and napthol AS-MX phosphate/fast blue BB (Sigma). The frequency of plasma cells specific for N protein was determined from the N protein-coated plates after background on the uncoated plates was subtracted.

Coronavirus neutralizing assay

Serum was inactivated by incubation at 56°C for 30 min. The known tissue culture infectious dose (TCID) of SARS-CoV was incubated for 1 h in the presence or absence of serum antibodies serially diluted 5-fold, and then added to Vero E6 cell culture grown confluently in a 96-well microtiter plate. After 48 h, cells were fixed with 10% formaldehyde and stained with crystal violet to visualize the cytopathic effect induced by the virus (14). Neutralization antibody titers were expressed as the minimum dilution number of serum that inhibited the cytopathic effect.

Western blotting

Purified SARS-CoV virion (0.5 μg) was fractionated on SDS-PAGE under reduced conditions. Proteins were transferred to PVDF membrane (Genetics, Tokyo, Japan) and reacted with the diluted sera (1:1000) that had been obtained from mice inoculated with UV-irradiated SARS-CoV. After washing, the membrane was reacted with HRP-conjugated $F(ab')_2$ fragment anti-mouse IgG (H+L) (1:20 000 Jackson Immuno Research, West Grove, PA), followed by visualization of the bands on X-ray film (Kodak, Rochester, NY) using chemiluminescent regents (Amasham Biosciences, Piscataway, NJ).

Regional T cell response

Popliteal and inguinal lymph nodes and spleens were harvested from mice 1 week after the boost vaccination. After the preparation of a single cell suspension, T cells were purified by depletion of $B220^+$, $Gr1^+$, $CD11b^+$, IgD^+ and IgM^+ cells using a magnetic cell sort system (MACS: Miltenyi Biotec, Bergisch Gladbach, Germany). To prepare antigen-presenting cells (APC), normal BALB/c mouse splenocytes were depleted of $CD3^+$ T cells by MACS and irradiated at 2000 cGy.

Purified T cells taken from lymph nodes (1×10^5 cells/well) were cultured with irradiated APC (5×10^5 cells/well) in the presence or absence of UV-irradiated purified SARS-CoV virion (1 or 10 μg/ml). Four days after the cultivation, the level of cytokine concentration in the culture supernatant was measured by flow cytometry using a mouse Th1/Th2 cytokine cytometric bead array kit (Becton Dickinson, San Jose, CA). T-cell proliferation was monitored by the incorporation of [^{3}H]thymidine (18.5 kBq/well, ICN Biomedicals, Costa Mesa, CA) added 8 h prior to cell harvest. The cells were harvested on a 96-well microplate bonded with a GF/B filter (Packard Instruments, Meriden, CT). Incorporated radioactivity was counted by a microplate scintillation counter (Packard Instruments).

Results

Inoculation with UV-inactivated SARS-CoV results in an antigen-specific IgG_1 response, probably by generating long-term ASCs as well as memory cells

To examine the level of anti-SARS-CoV response in mice after inoculation with vaccine candidates, three mice in each group were subcutaneously inoculated with 10 μg of UV-inactivated purified SARS-CoV with (Virion/Alum) or without alum (Virion), or inoculated with alum alone (Alum) or left untreated (None) as a control (Fig. 1). One month after inoculation, vaccinated mice elicited the anti-SARS CoV IgG antibody in sera at high levels. As expected, the alum adjuvant enhanced the level of IgG antibody response, >10-fold higher than the level without adjuvant (Fig. 1C compared with B). When mice were boosted at 7 weeks, the level of IgG antibody in both groups of mice was further increased ~10-fold above the primary response (Fig. 1B and C). Notably, the level of serum antibodies induced by a single injection of virion, even in the absence of the alum adjuvant, was maintained at least more than 6 months (Fig. 1D). These results suggest that long-term ASCs can be established by a single shot of UV-inactivated virion administration.

Upon restimulation with antigen, memory B cells rapidly differentiate into ASCs and migrate into the bone marrow to establish a long-term ASC pool (15,16). To enumerate the number of plasma cells specific for SARS-CoV, we performed an ELISPOT assay using recombinant N proteins, amino acid numbers 1–49 (N1–49) and 340–390 (N340–390) as coating antigens. Consistent with the serum anti-SARS CoV IgG level, SARS-specific IgG_1 plasma cells were maintained in the bone marrow at day 10 after boost immunization with virion/alum

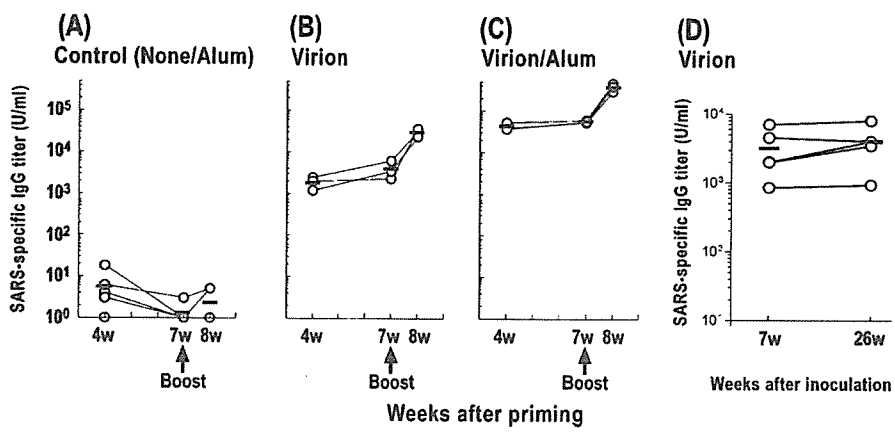

Fig. 1. The level of SARS-specific IgG in subcutaneously vaccinated mice. Mice were subcutaneously primed with 10 μg of UV-inactivated SARS-CoV virion (B), or virion with 2 mg of alum (C), or alum alone or none (A) and boosted with the same dose in their footpads at 7 weeks after priming. Serum was collected at the indicated time point and subjected to ELISA to detect SARS-specific IgG using SARS-CoV-infected Vero cell lysates as a coating antigen. Circles and bars represent the amount of IgG antibody in the serum of each mouse and the mean, respectively. The amount of IgG was arbitrarily calculated based on the concentration of hyper-immune sera. A representative result of two independent experiments is shown. (D) Mice were vaccinated with 10 μg of UV-inactivated SARS-CoV virion subcutaneously into their backs. Serum was collected from individual mice at the indicated time point and subjected to ELISA to detect SARS-specific IgG.

(Fig. 2). In contrast, the number of spots from control mice was below the detection limit (i.e. <1 ASC/9 × 10^5 cells).

UV-inactivated SARS-CoV induces IgG_1 antibody with neutralizing activity

We determined the subclass of serum anti-SARS-CoV IgG antibodies in the boosted mice using anti-mouse IgG_1, IgG_{2a}, IgG_{2b} or IgG_3 second antibody by ELISA (Fig. 3). Interestingly, the level of anti-SARS-CoV IgG_{2a} in mice immunized with virion/alum was comparable to that in mice immunized with virion alone, whereas the level of anti-SARS-CoV IgG_1 was higher in mice with virion/alum than the mice with virion alone. In contrast, the levels of IgG_{2b} and IgG_3 antibodies were fairly low in both groups. Therefore, our results indicated that vaccination with a combination of inactivated virion and alum induced a predominantly Th2-type immune response.

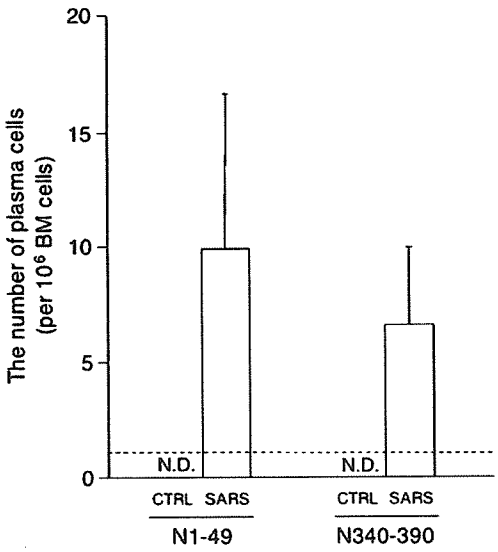

Fig. 2. The number of SARS-specific IgG_1 plasma cells in BM. Mice were primed and boosted by subcutaneous injection into their back with 10 μg of UV-inactivated SARS-CoV virion with 2 mg of alum (VA). BMs were collected at 10 days after boost and subjected to ELISPOT to detect SARS-specific IgG_1 plasma cells. Bars represent the number of plasma cells specific to N1–49 and N340–390 antigen in SARS-vaccinated and control mice, respectively. Data are means of triplicate cultures. The number of spots from control mice was below the detection limit (i.e. <1 ASC/9 × 10^5 cells: dashed line). A representative result of two independent experiments is shown. N.D.: not detected.

We also measured serum immunoglobulins other than IgG in the early and late phases of immunization. To avoid high IgG concentrations interfering with the detection of IgM and IgA antibodies, the serum IgG was absorbed with protein G-conjugated beads (>98%). The levels of anti-SARS-CoV IgM antibodies in the IgG-depleted sera, which were obtained 4 weeks after priming, were below our detection limit. Likewise, anti-SARS-CoV IgA antibody in the IgG-depleted sera, which were obtained 1 week after booster, was not detectable (data not shown).

Whether or not immune sera possess a neutralizing activity against SARS-CoV is a crucial aspect of vaccination. We estimated the neutralizing activity of sera obtained 1 week after boost inoculation (Table 1). We observed that neutralizing activity against SARS-CoV was detected at a high level in sera of mice inoculated with virion/alum or virion alone. Taken together, these results indicate that subcutaneous vaccination with UV-inactivated SARS-CoV virion is able to elicit a sufficient amount of IgG antibodies with neutralizing activity.

UV-inactivated SARS-CoV induces serum IgG antibody specific for S and N proteins

Using the immune sera of mice boosted with virion/alum 1 week before, we analyzed the specificity of serum IgG by western blot analysis (see Methods). As shown in Fig. 4(A), the robust signal detected at 50 kDa corresponds to the N protein of SARS-CoV, as predicted by its genome size (3,4). A band near 200 kDa appears to correspond to S protein, analogous with the S protein of other human coronaviruses, HCV-229E

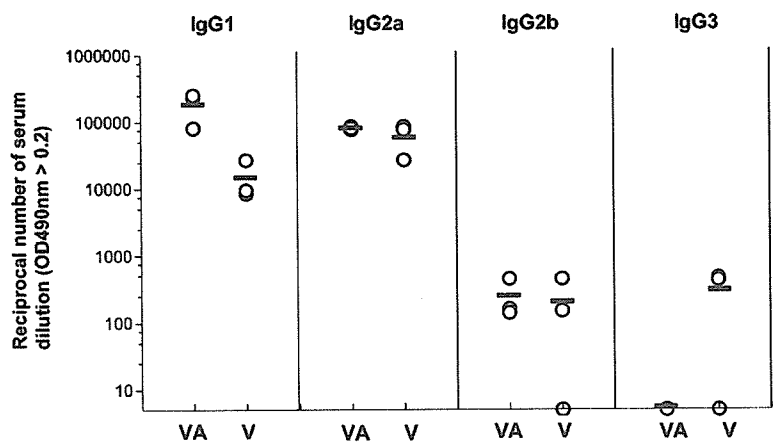

Fig. 3. IgG subclass of immunized serum. Mice were subcutaneously primed and boosted by injection in their footpads with 10 μg of UV-inactivated SARS-CoV virion (V), or virion with 2 mg of alum (VA). Serum was collected from individual mice at 1 week after boost and subjected to ELISA to detect SARS-specific IgG_1, IgG_{2a}, IgG_{2b} and IgG_3 titer. The Y value is the reciprocal serum dilution number where the OD490nm ≥ 0.2 in each ELISA. Circles and bars represent the titer for each mouse and the mean, respectively; results are representative of two separate experiments.

and HCV-OC43, which are known to be heavily glycosylated and detected at 186 kDa and 190 kDa, respectively (17). Our result is consistent with the data reported recently by Xiao *et al.* who expressed the full-length S glycoprotein of SARS-CoV Tor2 strain in 293 cells and showed that the protein ran ~180–200 kDa in SDS gels (18). The origins of the 120 kDa and the faint 37 kDa bands were unknown. However, similar bands were also detected on a fluorogram by using anti-N mAbs (Ohnishi, K., Sakaguchi, M., Takasuka, N. *et al.*, unpublished data), suggesting that it is related to N protein. The specificity of IgG in the immune sera was also determined by ELISA plates coated with lysates of cells infected with either S- or N-expressing recombinant vaccinia viruses (Fig. 4B). The results indicated that anti-S as well as anti-N protein IgG antibodies were elicited by virion/alum vaccination.

Table I. Neutralizing activity in serum after vaccination

		Reciprocal endpoint titer	
		Experiment 1	Experiment 2
None/alum		<5*	<5*
Virion	mouse 1	250	250
	2	1250	250
	3	1250	250
Virion/alum	1	250	1250
	2	1250	1250
	3	1250	1250

*All six mice examined did not have detectable neutralizing activity. Sera were obtained from mice 1 week after boost vaccination and subjected to SARS-CoV neutralizing activity assay as described in Methods. The titer is a reciprocal number of minimum serum dilution that inhibits the cytopathic effect.

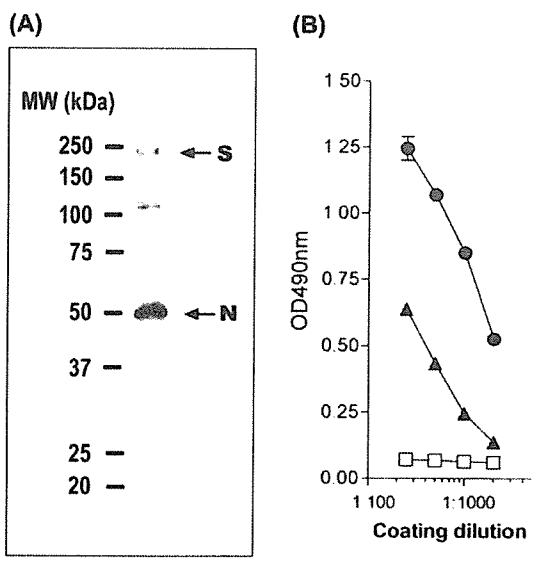

Fig. 4. Specificity of the serum antibodies. (A) Purified UV-inactivated SARS-CoV virion (0.5 μg) was fractionated by SDS–PAGE and subjected to western blotting. Diluted pooled sera (1:1000) from mice primed and boosted with virion/alum were exploited to detect virus proteins. Upper and lower arrows indicate the predicted band of S (spike protein) and N (nucleocapside protein) of SARS-CoV, respectively. The size of molecular weight markers (kDa) is shown on the left. (B) S protein- or N protein-specific ELISA. ELISA plates were coated at the indicated dilution with 1% NP40 lysates of chick embryo fibroblasts that had been infected with S protein-expressing vaccinia virus (circle), N protein-expressing vaccinia virus (triangle) or uninfected (mock; square). Diluted serum (1:1000) from mice prime and boost immunized with virion/alum, was exploited for detection of virus proteins.

UV-inactivated SARS-CoV whole virion induces T-cell response

To examine whether or not subcutaneously vaccinated mice gained an induced T-cell response against SARS-CoV, mice were immunized either with virion/alum, virion, or alum only via the footpad. T cells of these mice were enriched from the spleen and regional lymph nodes 1 week after a booster immunization and cultured with irradiated APCs in the presence or absence of UV-inactivated SARS-CoV virion at 1 or 10 μg/ml. As shown in Fig. 5(A), regional lymph node T cells proliferated *in vitro* in response to UV-inactivated virion in virion/alum-immunized mice and, to a lesser extent, in virion-immunized mice. Because mice inoculated with virion/alum showed a high basal level of proliferation of lymph node T cells in the absence of antigen, there is not much difference in the net proliferative response of these cells between the virion/alum group and the virion only group. On the other hand, in splenic T cells, a low level of proliferation was observed only in the virion/alum group of mice. The level of proliferation of these T cells, however, was virion-dose independent. Therefore, our results suggest that the subcutaneous injection of inactivated virion, even without alum, does induce T cell activation to some extent in the draining lymph node, a result which hardly occurs systemically.

We also measured the level of cytokine production in the supernatant of lymph node T cells stimulated with inactivated virion *in vitro* for 4 days. We found that the inactivated virion induced the production of all the cytokines (IL-2, IL-4, IL-5, IFN-γ and TNF-α) in T cells of virion/alum-immunized mice, in a dose-dependent manner (Fig. 5B). Likewise, T cells of virion-immunized mice produced low, yet significant, levels of these cytokines in a dose-dependent manner, except IL-5. In contrast, lymph node T cells from normal mice did not produce any cytokines at all in response to virion, suggesting that the virion itself does not possess innate stimulating activity as bacterial products [such as lipopolysaccharide (LPS) and purified protein derivative of mycobacterium tuberculosis (PPD)] do. Taken together, these results suggest that subcutaneous vaccination with UV-inactivated SARS-CoV is able to activate $CD4^+$ T cells in regional lymph nodes, where T cells produce several immunoregulatory cytokines, including IFN-γ.

Discussion

The present results demonstrated that even a single subcutaneous administration of UV-irradiated virion without alum adjuvant induced a high level of systemic anti-SARS-CoV antibody response in mice, probably followed by the generation of long-term antibody-secreting cells and memory cells in the bone marrow. Considering that polyvalent particulate

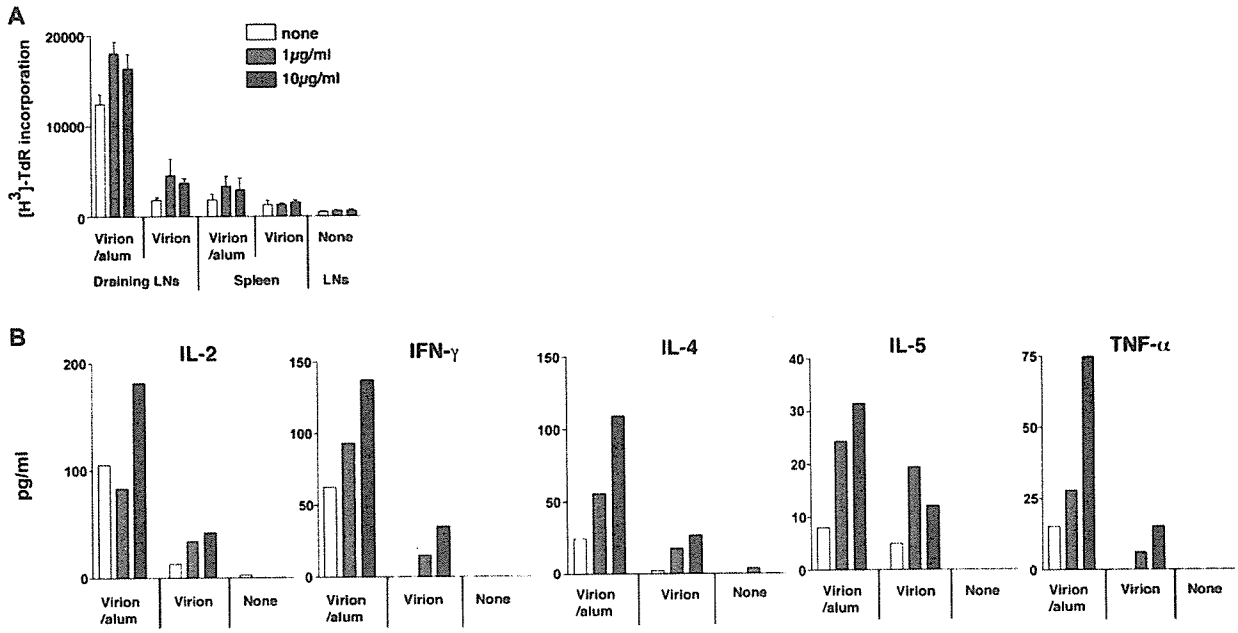

Fig. 5. *In vitro* responses of SARS-CoV-specific T cells taken from mice vaccinated with inactivated SARS-CoV. Mice were subcutaneously primed with 10 μg of UV-inactivated SARS-CoV virion, or virion with 2 mg of alum, or none, and then boosted with the same dose in their footpads at 7 weeks after priming. Draining lymph nodes and spleens were isolated at 1 week after boost and stimulated with T-cell depleted splenocytes that had been pulsed with the indicated concentration of UV-inactivated SARS-CoV virion. These cells were cultured for 2–4 days and [^{3}H]thymidine was added 8 h prior to the harvest. The peak response on day 4 after cultivation is shown in (A). (B) Culture supernatant was collected at day 2–4 post cultivation and the level of IL-2, IFN-γ, IL-4, IL-5 and TNF-α was determined by CBA kit. The maximum cytokine production at day 4 is shown. Results are representative of two separate experiments.

structures such as hepatitis B virus surface antigen-based, HIV-1 Gag-based and Ty virus-like particles have been shown to elicit humoral as well as cellular immune responses (19), these particulates probably have comparable dimensions and structures to the pathogens that are targeted for uptake by APCs to facilitate the induction of potent immune responses. The antibodies elicited in mice vaccinated by the current protocol with or without adjuvant recognized both the S and N proteins of SARS-CoV and were able to neutralize the infection of virus to Vero E6 cells. However, serum anti-SARS-CoV IgA antibody was not detectable, probably owing to the route of vaccination. In addition, the present vaccination protocol caused T cell response at the regional lymph nodes, although it did not allow for the induction of a sufficient cellular immune response systemically.

We show here the potentiality of subcutaneous injection of inactivated virion with alum, which is utilized for most of current human vaccinations. Alum has been used as an adjuvant for vaccines such as diphtheria, pertussis and tetanus, and these vaccines have a long safety record for human use (20). We observed that the addition of alum to the vaccine formula resulted in a large augmentation of serum IgG_1 production, but not IgG_{2a} production. The level of IgG_1 in alum-vaccinated mice reached a level similar to that found in hyper-immunized mice, which were subcutaneously injected with 5 μg of inactivated virion emulsified with a complete Freund adjuvant, followed by consecutive three-times intravenous boosters with 2 μg of virion. Alum is known to selectively stimulate an IgG_1 dominant, type 2 immune response [reviewed in (21)]. Activation of complement by alum could contribute to the type 2-biased immune response partly via an inhibition of IL-12 production. Interestingly, a quite recent report demonstrated that an alum-induced $Gr1^+$ myeloid cell population produced IL-4 and activated B-cells (22).

There are various diseases associated with animal coronavirus infection. The clinical manifestations of the disease and the correlates of protection with immunity have been studied extensively in these animal coronavirus infections [reviewed in (7)]. Although antibodies and T cells may play a role in exacerbating the pathology in some animal coronavirus infections (23,24), both humoral and cellular immune responses are known to contribute to protection against coronavirus infection. In murine hepatitis virus, a Group 2 coronavirus, the mortality of susceptible mice was partially prevented by the transfer of immune serum containing neutralizing antibody prior to challenge (25). Recently, Zhi-yong *et al.* reported in the murine acute infection model that the neutralizing antibody elicited by vaccination of DNA encoding S was protective, but cellular components of vaccinated mice were not required for the inhibition of viral replication (26). Because a twice parenteral administration of inactivated virion with alum induced a high level of antibodies that are able to neutralize SARS-CoV, this vaccination protocol may have a certain effect on the protection of humans from SARS-CoV infection.

We observed that two successive inoculations with inactivated virus at 7 week intervals generated SARS-CoV-specific

T cells. These cells were restimulated with the irradiated virus *in vitro*, but their response was low in terms of the level of proliferation and production of INF-γ and IL-2. However, irrespective of vaccination protocols with or without alum adjuvant, virus-primed T cells of vaccinated animals were capable of producing IL-4 at high levels upon *in vitro* stimulation, comparable to other reports for a variety of vaccination studies (27,28). This outlook seems compatible with the idea that the present vaccine protocol may tend to select T-cell subsets with Th2 phenotype. However, it remains to be elucidated whether such T cells may exhibit serological memory phenotype and persist in the immune system after vaccination as long as memory B cells, which may persist more than 180 days post vaccination. In addition, further analysis is needed to clarify whether T cell response is a crucial factor for long-term protection against SARS-CoV infections.

Efforts to develop a SARS-CoV vaccine have been carried out by many profitable or non-profitable organizations in various ways. For example, it has recently been reported that the combination of adenovirus vector expressing SARS-S, -M or -N protein elicited a neutralizing capacity in serum and N-specific T-cell response in rhesus macaques (29). However, it is still uncertain whether or not the immunity against only these components of SARS-CoV is sufficient for virus protection. SARS-CoV tends to cause replication errors, which may allow the virus to escape the host-immune response and result in a seasonal outbreak. From this point of view, it resembles influenza virus. In influenza virus, inactivated HA vaccine showed incomplete protection but had a certain efficacy and safety record for a long period of time. Indeed, this approach has been used in the veterinary field, such as with the bovine coronavirus (30) and canine coronavirus (31). These advantages make a whole killed virion a prime candidate for a SARS vaccine, even if it may not have the best protective ability.

Unfortunately, no information is available so far on the immune correlates of protection against human coronaviruses, including SARS-CoV. In consideration that SARS-CoV transmission occurs by direct contact with droplets or by the fecal oral route, mucosal secretary IgA in both the lower respiratory tract and digestive tract seem to be crucially important. Failure to induce IgA-type antibodies in a current systemic vaccination method should be improved. Notably, IgA antibodies were detectable in the sera and bronchoalveolar lavage fluid obtained from mice hyper-immunized with UV-irradiated virus (data not shown). Therefore, if a non-toxic and more potent adjuvant becomes available for human use, the subcutaneous injection of inactivated virion would become an effective vaccination method to reduce the number of susceptible people.

In the future, it will be necessary to determine whether or not the inactivated whole virion vaccine possesses protective ability against SARS-CoV infection by the use of adequate animal models. Furthermore, whether the alum addition augmented the protection and the effective period of SARS-CoV virion vaccination should be addressed, because currently used inactivated influenza virus whole virion vaccine is significantly effective without any adjuvant. Meanwhile, we also need to develop a potent adjuvant for induction of a much stronger mucosal immunity, in addition to evaluating available methods of virion inactivation.

Acknowledgements

We thank Ms R. Ishida, Ms Y. Kaburagi and Mr Y. Kimishima for their excellent technical help. This work was supported by a grant from the Ministry of Public Health and Labor of Japan.

Abbreviations

ACE2	angiotensin-converting enzyme 2
ASC	antibody-secreting cell
E	envelope
M	membrane
N	nucleocapsid protein
SARS	severe acute respiratory syndrome
SARS-CoV	SARS-associated coronavirus
S	spike protein

References

1 Drosten, C., Gunther, S., Preiser, W. *et al.* 2003. Identification of a novel coronavirus in patients with severe acute respiratory syndrome. *N. Engl. J. Med.* 348:1967.
2 Ksiazek, T. G., Erdman, D., Goldsmith, C. S. *et al.* 2003. A novel coronavirus associated with severe acute respiratory syndrome. *N. Engl. J. Med.* 348:1953.
3 Marra, M. A., Jones, S. J., Astell, C. R. *et al.* 2003. The genome sequence of the SARS-associated coronavirus. *Science* 300:1399.
4 Rota, P. A., Oberste, M. S., Monroe, S. S. *et al.* 2003. Characterization of a novel coronavirus associated with severe acute respiratory syndrome. *Science* 300:1394.
5 Holmes, K. V. and Enjuanes, L. 2003. Virology. The SARS coronavirus: a postgenomic era. *Science* 300:1377.
6 Liu, X., Shi, Y., Li, P., Li, L., Yi, Y., Ma, Q. and Cao, C. 2004. Profile of antibodies to the nucleocapsid protein of the severe acute respiratory syndrome (SARS)-associated coronavirus in probable SARS patients. *Clin. Diagn. Lab. Immunol.* 11:227.
7 De Groot, A. S. 2003. How the SARS vaccine effort can learn from HIV—speeding towards the future, learning from the past. *Vaccine* 21:4095.
8 Li, W., Moore, M. J., Vasilieva, N. *et al.* 2003. Angiotensin-converting enzyme 2 is a functional receptor for the SARS coronavirus. *Nature* 426:450.
9 Collins, R. A., Knobler, R. L., Powell, H. and Buchmeier, M. J. 1982. Monoclonal antibodies to murine hepatitis virus-4 (strain JHM) define the viral glycoprotein responsible for attachment and cell–cell fusion. *Virology* 119:358.
10 Fleming, J. O., Stohlman, S. A., Harmon, R. C., Lai, M. M., Frelinger, J. A. and Weiner, L. P.1983. Antigenic relationship of murine coronaviruses: analysis using monoclonal antibodies to JHM (MHV-4) virus. *Virology* 131:296.
11 Jackwood, M. W. and Hilt, D. A. 1995. Production and immunogenicity of multiple antigenic peptide (MAP) constructs derived from the S1 glycoprotein of infectious bronchitis virus (IBV). *Adv. Exp. Med. Biol.* 380:213.
12 Anton, I. M., Gonzalez, S., Bullido, M. J., Corsin, M., Risco, C., Langeveld, J. P. and Enjuanes, L. 1996. Cooperation between transmissible gastroenteritis coronavirus (TGEV) structural proteins in the *in vitro* induction of virus-specific antibodies. *Virus Res.* 46:111.
13 Ishii, K., Ueda, Y., Matsuo, K. *et al.* 2002. Structural analysis of vaccinia virus DIs strain: application as a new replication-deficient viral vector. *Virology* 302:433.
14 Storch, G. A. 2001. Diagnostic virology. In Knipe, D. M., Howley, P. M., ed., *Fields Virology*, 4th edn. Lippincott Williams & Wilkins, Philadelphia, PA. pp. 493–531.
15 Benner, R., Hijmans, W. and Haaijman, J. J. 1981. The bone marrow: the major source of serum immunoglobulins, but still a neglected site of antibody formation. *Clin. Exp. Immunol.* 46:1.
16 Slifka, M. K., Matloubian, M. and Ahmed, R. 1995. Bone marrow is a major site of long-term antibody production after acute viral infection. *J. Virol.* 69:1895.
17 Schmidt, O. W. and Kenny, G. E. 1982. Polypeptides and functions of antigens from human coronaviruses 229E and OC43. *Infect. Immun.* 35:515.

18 Xiao, X., Chakraborti, S., Dimitrov, A. S., Gramatikoff, K. and Dimitrov, D. S. 2003. The SARS-CoV S glycoprotein: expression and functional characterization. *Biochem. Biophys. Res. Commun.* 312:1159.
19 Singh, M. and O'Hagan, D. 1999. Advances in vaccine adjuvants. *Nat. Biotechnol.* 17:1075.
20 Clements, C. J. and Griffiths, E. 2002. The global impact of vaccines containing aluminium adjuvants. *Vaccine* 20 (Suppl. 3): S24.
21 HogenEsch, H. 2002. Mechanisms of stimulation of the immune response by aluminum adjuvants. *Vaccine* 20 (Suppl. 3): S34.
22 Jordan, M. B., Mills, D. M., Kappler, J., Marrack, P. and Cambier, J. C. 2004. Promotion of B cell immune responses via an alum-induced myeloid cell population. *Science* 304:1808.
23 Weiss, R. C. and Scott, F. W. 1981. Antibody-mediated enhancement of disease in feline infectious peritonitis: comparisons with dengue hemorrhagic fever. *Comp. Immunol. Microbiol. Infect. Dis.* 4:175.
24 Wu, G. F., Dandekar, A. A., Pewe, L. and Perlman, S. 2001. The role of CD4 and CD8 T cells in MHV-JHM-induced demyelination. *Adv. Exp. Med. Biol.* 494:341.
25 Pope, M., Chung, S. W., Mosmann, T., Leibowitz, J. L., Gorczynski, R. M. and Levy, G. A. 1996. Resistance of naive mice to murine hepatitis virus strain 3 requires development of a Th1, but not a Th2, response, whereas pre-existing antibody partially protects against primary infection. *J. Immunol.* 156:3342.
26 Yang, Z. Y., Kong, W. P., Huang, Y., Roberts, A., Murphy, B. R., Subbarao, K. and Nabel, G. J. 2004. A DNA vaccine induces SARS coronavirus neutralization and protective immunity in mice. *Nature* 428:561.
27 Mazumdar, T., Anam, K. and Ali N. 2004. A mixed Th1/Th2 response elicited by a liposomal formation of *Leishmania* vaccine instructs Th1 responses and resistance to *Leishmania donovani* in susceptible BALB/c mice. *Vaccine* 22:1162.
28 Nicollier-Jamot, B., Ogier, A., Piroth, L., Pothier, P. and Kohli, E. 2004. Recombinant virus-like particles of a norovirus (genogroup II strain) administered intranasally and orally with mucosal adjuvants LT and LT(R192G) in BALB/c mice induce specific humoral and cellular Th1/Th2-like immune responses. *Vaccine* 22:1079.
29 Gao, W., Tamin, A., Soloff, A., D'Aiuto, L., Nwanegbo, E., Robbins, P. D., Bellini, W. J., Barratt-Boyes, S. and Gambotto, A. 2003. Effects of a SARS-associated coronavirus vaccine in monkeys. *Lancet* 362:1895.
30 Takamura, K., Matsumoto, Y. and Shimizu, Y. 2002. Field study of bovine coronavirus vaccine enriched with hemagglutinating antigen for winter dysentery in dairy cows. *Can. J. Vet. Res.* 66:278.
31 Pratelli, A., Tinelli, A., Decaro, N., Cirone, F., Elia, G., Roperto, S., Tempesta, M. and Buonavoglia, C. 2003. Efficacy of an inactivated canine coronavirus vaccine in pups. *New Microbiol.* 26:151.

Available online at www.sciencedirect.com
SCIENCE DIRECT®
ELSEVIER
Biochemical and Biophysical Research Communications 318 (2004) 719–725
BBRC
www.elsevier.com/locate/ybbrc

HIV protease inhibitor nelfinavir inhibits replication of SARS-associated coronavirus

Norio Yamamoto,[a] Rongge Yang,[a] Yoshiyuki Yoshinaka,[a] Shinji Amari,[b] Tatsuya Nakano,[c] Jindrich Cinatl,[d] Holger Rabenau,[d] Hans Wilhelm Doerr,[d] Gerhard Hunsmann,[e] Akira Otaka,[f] Hirokazu Tamamura,[f] Nobutaka Fujii,[f] and Naoki Yamamoto[a,*]

[a] *Department of Molecular Virology, Bio-Response, Graduate School, Tokyo Medical and Dental University, 1-5-45 Yushima, Bunkyo-ku, Tokyo 113-8519, Japan*
[b] *Collaborative Research Center of Frontier Simulation Software for Industrial Science, Institute of Industrial Science, University of Tokyo, 4-6-1 Komaba, Meguro-ku, Tokyo 153-8505, Japan*
[c] *Division of Safety Information on Drug, Food, and Chemicals, National Institute of Health Sciences, 1-18-1 Kamiyoga, Setagaya-ku, Tokyo 158-8501, Japan*
[d] *Institute of Medical Virology, Frankfurt University Medical School, Paul-Ehrlich Str 40, D-60596 Frankfurt, Germany*
[e] *Department of Virology and Immunology, German Primate Center, Kellnerweg 4, D-37077 Gottingen, Germany*
[f] *Graduate School of Pharmaceutical Sciences, Kyoto University, Sakyo-ku, Kyoto 606-8501, Japan*

Received 7 April 2004
Available online 6 May 2004

Abstract

A novel coronavirus has been identified as an etiological agent of severe acute respiratory syndrome (SARS). To rapidly identify anti-SARS drugs available for clinical use, we screened a set of compounds that included antiviral drugs already in wide use. Here we report that the HIV-1 protease inhibitor, nelfinavir, strongly inhibited replication of the SARS coronavirus (SARS-CoV). Nelfinavir inhibited the cytopathic effect induced by SARS-CoV infection. Expression of viral antigens was much lower in infected cells treated with nelfinavir than in untreated infected cells. Quantitative RT-PCR analysis showed that nelfinavir could decrease the production of virions from Vero cells. Experiments with various timings of drug addition revealed that nelfinavir exerted its effect not at the entry step, but at the post-entry step of SARS-CoV infection. Our results suggest that nelfinavir should be examined clinically for the treatment of SARS and has potential as a good lead compound for designing anti-SARS drugs.
© 2004 Elsevier Inc. All rights reserved.

Keywords: Severe acute respiratory syndrome; Coronavirus; HIV protease inhibitor

Severe acute respiratory syndrome (SARS) is an emerging disease that was first reported in Guangdong Province, People's Republic of China, in November, 2002. Since then, SARS has spread to 32 countries and has resulted in more than 800 deaths from respiratory distress syndrome [1–3]. An overall estimate of case fatality reached 14–15% as reported by WHO [4] and the mortality rate in people older than 60 years could be as high as 43–55% [5].

* Corresponding author. Fax: +81-3-5803-0124.
E-mail address: yamamoto.mmb@tmd.ac.jp (N. Yamamoto).

0006-291X/$ - see front matter © 2004 Elsevier Inc. All rights reserved.
doi:10.1016/j.bbrc.2004.04.083

Several groups, including the authors, isolated a novel coronavirus from SARS patients [2,6,7]. It has been shown that SARS-CoV satisfies Koch's postulates for causation—its consistent isolation from patients suffering from SARS, isolation of the virus and reproduction of disease in non-human primates after inoculation, and the presence of a specific antibody response against the virus in both SARS patients and artificially infected primates [8]. Now its etiological role in SARS is widely accepted.

The outbreak of SARS in several countries has led to the search for active antiviral compounds and vaccines for this disease [9]. Although the results of many clinical

experiments have been reported, no consensus on treatment has been reached to date. Therapeutic protocols with steroids and ribavirin have been widely used empirically from the outset of the epidemic [10,11]. The use of steroids for SARS seemed beneficial, whenever they are appropriately applied. However, the optimal timing, dosage, and duration of treatment have not yet been determined. On the other hand, the administration of ribavirin did not apparently reduce either the rate of intratracheal intubation or that of mortality [12]. Moreover, significant toxicity, such as hemolytic anemia, has been attributed to ribavirin [13]. A few preliminary trials and in vitro data suggested the possibility of treating SARS with interferon [14–16]. Other agents including glycyrrhizin and convalescent plasma require further studies [17]. As is well established in the case of HIV-1 infection, the combination of antiviral drugs will make it possible to establish a better protocol for the treatment of SARS.

To identify anti-SARS drugs available for clinical use as rapidly as possible, we screened a set of compounds including antiviral drugs already in human clinical use. We found that nelfinavir, a widely used HIV-1 protease inhibitor, could inhibit SARS-CoV replication efficiently. Our results suggest that nelfinavir should be examined clinically for the treatment of SARS.

Materials and methods

Cell culture and virus. Vero E6 cells were maintained in Dulbecco's modified Eagle's medium supplemented with 10% FBS and glutamine–penicillin–streptomycin solution in 5% CO_2 in humidified air at 37 °C.

The FFM-1 strain of SARS-CoV was isolated from a SARS patient admitted to the Clinical Centre of Frankfurt University. This strain was used in all experiments to assess the antiviral activity of the drugs.

Compounds for screening. A set of compounds for screening consisted of 24 drugs as follows: nelfinavir, saquinavir, KNI-272, TYA5, TYB5, ritonavir, lopinavir, indinavir, 4F-benzoyl-TN14003, 4F-benzoyl-TE14011, TN14003, T140, TC14012, FC131, T22, SDF-1, vMIP-II, TAK-779, SC34, N36, T-20, glycyrrhizin, glycyrrhetic acid, and Cardran sulfate.

Cytopathic effect assay. SARS-CoV was inoculated into a monolayer of Vero E6 cells in 24-well plates at a multiplicity of infection (MOI) of 0.01. The plates were incubated at 37 °C in 5% CO_2 for 3 days and CPE in each well was observed.

Immunofluorescence assay. The Vero E6 cells in 24-well plates were infected with SARS-CoV at the MOI of 0.01. The infected cells were fixed with methanol 24 h after infection and incubated at room temperature for 1 h with diluted serum sample from a SARS patient. After washing with PBS, the cells were incubated with anti-human-IgG antibody conjugated with FITC for 30 min at room temperature. The cells were washed with PBS, mounted in buffered glycerol, cover-slipped, and viewed with a fluorescence microscope.

RNA extraction and real-time RT-PCR assay. SARS-CoV RNA in the culture supernatant was purified with ISOGEN (Nippongene) according to the manufacturer's protocol. For quantification of SARS-CoV ORF-1 RNA, we performed real-time RT-PCR with the primers and the probe as follows: ORF1-F, AGCTACGAGCACCAGACACC; ORF1-R, ACTTTGGGCATTCCCCTTT; ORF1-probe, TCGAAA TTAAGAGTGCCAAGAAATTTGACACTTT. The fluorescence intensity generated from the probe was detected by the ABI-7700 sequence detector system (Applied Biosystems).

MTT assay. Vero E6 cells in 96-well plates were infected with SARS-CoV at the MOI of 0.01. After 36 h of culture, cells were incubated for 4 h in the presence of 0.5 mg/ml of 3-(4,5-dimethylthiazol-2-yl)-2,5-diphenyl tetrazolium bromide (MTT). Formazan crystals were dissolved with 100 μL of 0.04 N HCl-isopropyl alcohol (acid isopropanol) and absorbance at 570 nm was measured with a reference wavelength of 655 nm.

Time-of-addition experiments. Drugs, including nelfinavir, were added to cultures of Vero E6 cells at the time of infection or 3 h after infection. Samples were processed for a quantitative RT-PCR assay and an immunofluorescence assay 24 h after infection. The cytopathic effect of infected cells was analyzed 36 h after infection.

Entry inhibition assay. Vero E6 cells were pretreated with each drug for 3 h, and SARS-CoV was inoculated at the MOI of 0.1. Cells and viruses were incubated for 3 h and washed with PBS three times. Subsequently, infected cells were lysed with ISOGEN (Nippongene) and RNA was purified according to the manufacturer's protocol. Extracted RNA samples were subjected to real-time RT-PCR analysis for quantification of SARS-CoV RNA as described above. As a loading control for normalization, 18S ribosomal RNA was quantified with the primers and the probe as follows: 18S-F, GTAACCCGTTGAACCCCATT; 18S-R, CCATCCAATCGGTAGTAGCG; and 18S-probe, TGCGTT GATTAAGTCCCTGCCCTTTGTA.

Results and discussion

Nelfinavir inhibited replication of SARS-CoV

We screened our chemical library and found that nelfinavir could inhibit SARS-CoV replication in Vero E6 cells. Nelfinavir clearly inhibited the cytopathic effect (CPE) induced by infection with SARS-CoV (Fig. 1A). We also examined the replication of SARS-CoV by immunofluorescence assay (IFA) with a serum sample from a patient with SARS. Expression of viral antigens was much lower in infected cells treated with nelfinavir than in untreated infected cells (Fig. 1B). Furthermore, we assessed the effect of nelfinavir on the production of virions. Nelfinavir significantly blocked the production of virions as revealed by quantitative RT-PCR (Fig. 2). By the use of MTT assay, we determined the concentration of the compound that reduced cell viability to 50% (CC_{50}), the concentration of the compound required for inhibition of CPE to 50% of the control value (EC_{50}), and the selectivity index (SI). Nelfinavir inhibited SARS-CoV replication at non-toxic doses with an approximate SI of 300, while the other inhibitors against HIV-1 protease (ritonavir, lopinavir, saquinavir, indinavir, TYA5, TYB5, and KNI-272) did not affect the replication of SARS-CoV (Table 1). These results revealed that nelfinavir is active in inhibiting SARS-CoV replication.

Nelfinavir inhibited SARS-CoV replication at the post-entry, but not the entry step

To disclose the step at which nelfinavir affects the virus life cycle, we performed time-of-addition experiments on the replication of SARS-CoV.

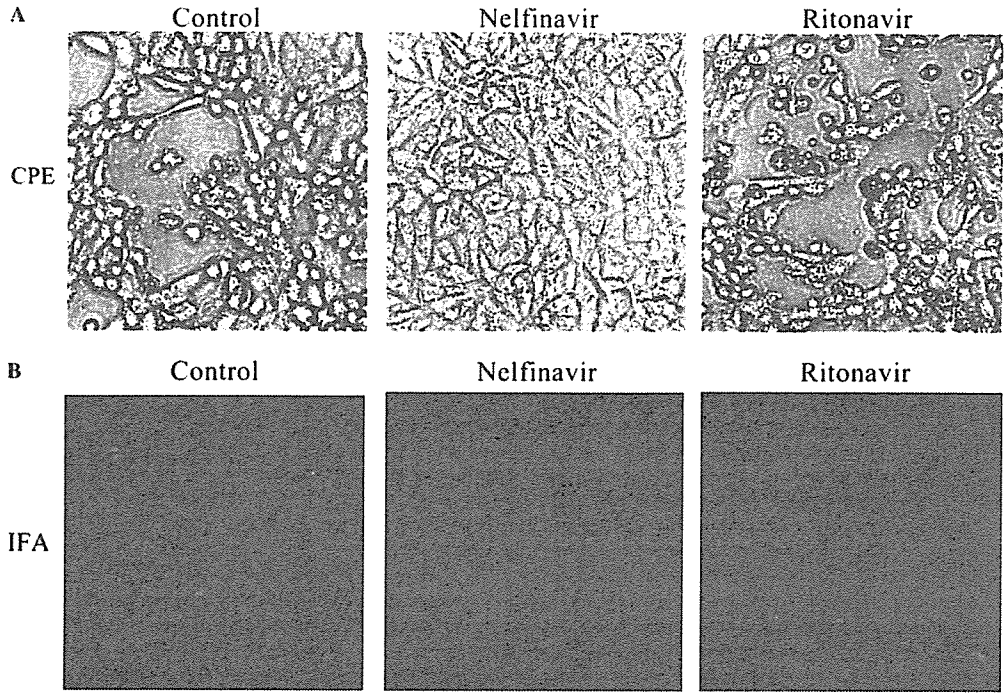

Fig. 1. Effect of nelfinavir on replication of SARS-CoV in Vero E6 cells. (A) Cytopathic effect (CPE) in Vero E6 cells. The cells were treated with phosphate-buffered saline (PBS) as a control, 10 μM nelfinavir, or 10 μM ritonavir for 3 h before infection. CPE was observed 36 h after infection. (B) Immunofluorescence assay (IFA) of infected cells treated with PBS, 10 μM nelfinavir, or 10 μM of ritonavir. Cells were fixed with methanol 24 h after infection and stained with serum samples from SARS patients.

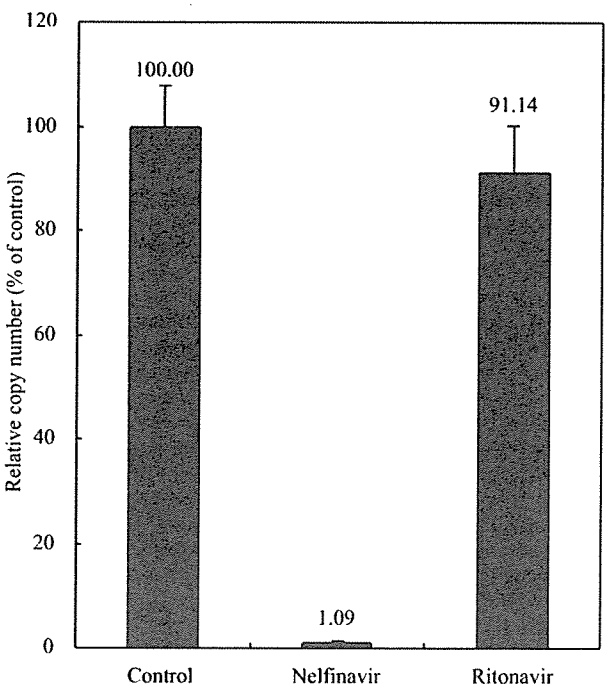

Fig. 2. Real-time RT-PCR for SARS-CoV RNA. Vero E6 cells had been treated with nelfinavir or ritonavir for 3 h before infection at the concentration of 10 μM. Instead of these drugs, PBS was added as a negative control. Viral RNA in the culture supernatant was collected 24 h after infection and quantified by the use of a fluorogenic probe. All samples were analyzed in triplicate.

Table 1
Activity of compounds against SARS-associated coronavirus in Vero cell cultures

Compound	EC_{50} (μM)	CC_{50} (μM)	Selectivity index
Nelfinavir	0.048 (0.024)	14.5 (2.75)	302.1
Saquinavir	NC	31.4 (7.82)	NC
KNI-272	NC	8.85 (2.05)	NC
TYA5	NC	16.3 (3.13)	NC
TYB5	NC	9.22 (2.25)	NC
Ritonavir	NC	13.8 (2.94)	NC
Lopinavir	NC	24.15 (5.01)	NC
Indinavir	NC	9.63 (3.11)	NC

NC, not calculable.

EC_{50}, effective concentration of compound needed to inhibit the cytopathic effect to 50% of control value.

CC_{50}, cytotoxic concentration of the compound that reduced cell viability to 50%.

Mean (standard error) of three assays was calculated for each drug.

Nelfinavir significantly inhibited SARS-CoV replication when used before infection (Figs. 1A and B and 2). When this drug was added at the time of infection or 3 h after infection, it was still able to block the CPE induced by SARS-CoV infection (Fig. 3A). Addition of nelfinavir at various timings inhibited the expression of viral antigens in Vero cells as shown by IFA (Fig. 3B). Nelfinavir blocked the production of virions when used to treat the cells at the time of infection or 3 h after infection (Fig. 4). The other protease inhibitors including ritonavir had no effect on replication of SARS-CoV

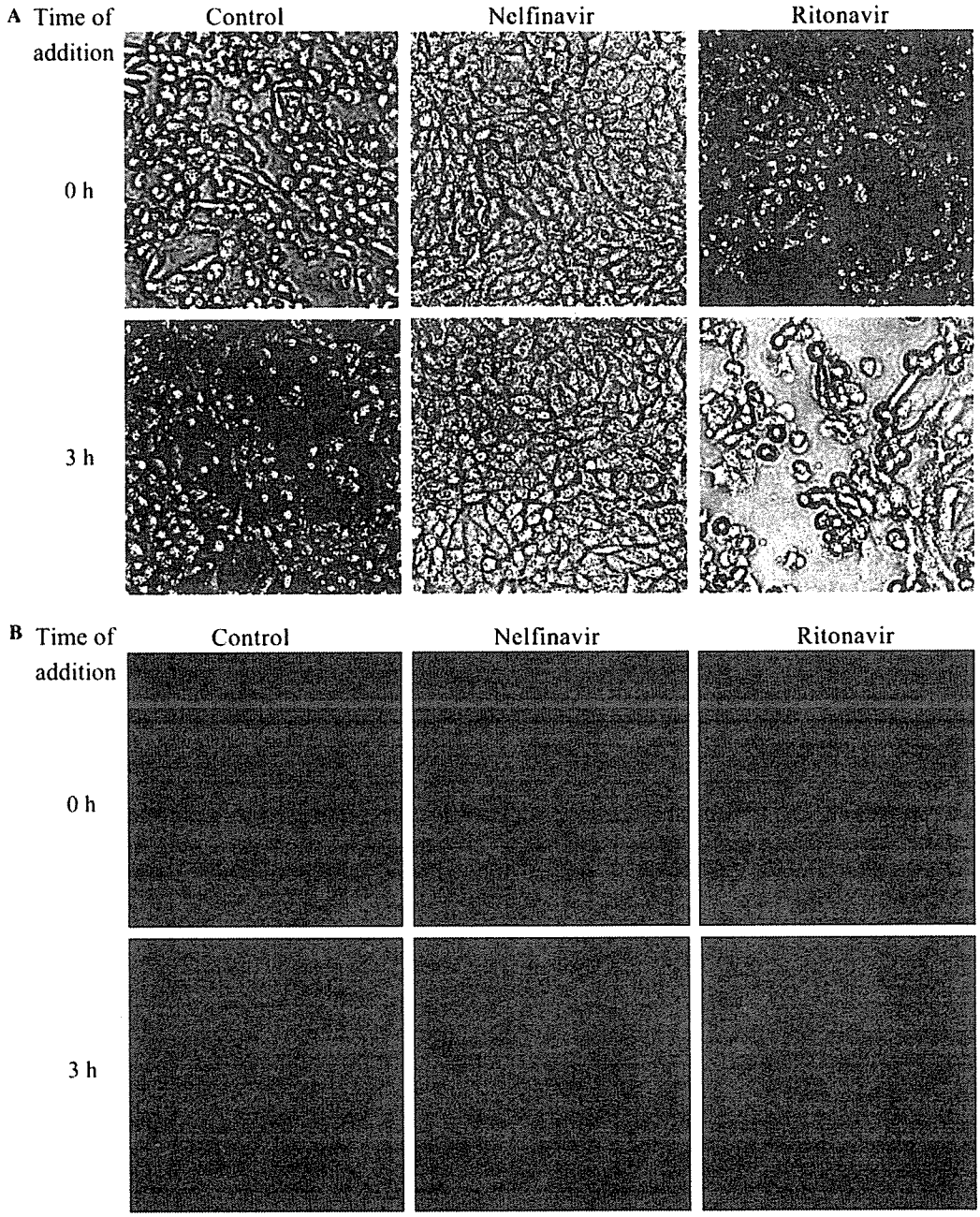

Fig. 3. Effect of various timings of drug addition on SARS-CoV replication in Vero E6 cells. (A) CPE in Vero E6 cells when drugs were added at the time of infection or 3 h after infection. The cells were treated with phosphate-buffered saline (PBS) as a control, 10 μM nelfinavir, or 10 μM ritonavir and CPE was observed 36 h after infection. (B) IFA of infected cells when drugs were added at the time of infection or 3 h after infection. The cells were treated with PBS as a control, 10 μM nelfinavir, or 10 μM ritonavir. The cells were fixed with methanol 24 h after infection and stained with serum samples from SARS patients.

(Figs. 3A and B and 4). These results indicate that the target(s) of nelfinavir may be involved in the post-entry step of SARS-CoV replication.

To investigate whether or not nelfinavir can affect the efficiency of virion entry, we quantified the copy number of SARS-CoV RNA in Vero cells immediately after the entry of virions.

Real-time RT-PCR revealed that nelfinavir did not affect the entry step of SARS-CoV infection (Fig. 5), which is consistent with our assumption that nelfinavir blocks the post-entry step of SARS-CoV replication.

The mechanisms that underlie the inhibitory action of nelfinavir on SARS-CoV replication remain to be identified. The main proteinase of SARS-CoV is one of

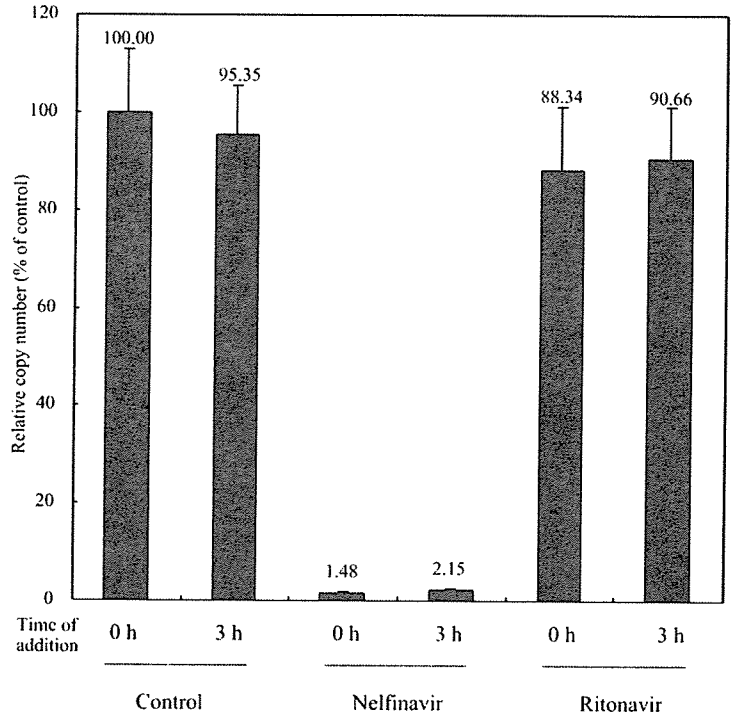

Fig. 4. Real-time RT-PCR for SARS-CoV RNA with various timings of drug addition. Nelfinavir or ritonavir was added at the time of infection or 3 h after infection at the concentration of 10 μM. Instead of these drugs PBS was added as a negative control. Viral RNA in the culture supernatant was collected 24 h after infection and quantified by the use of a fluorogenic probe. All samples were analyzed in triplicate.

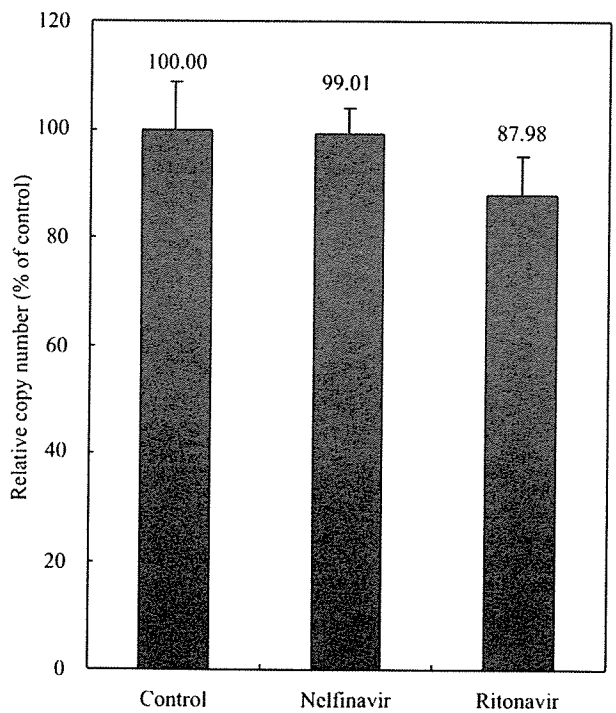

Fig. 5. Entry inhibition assay. To quantify SARS-CoV RNA which entered the cells. Vero E6 cells were pretreated with the drugs and infected with SARS-CoV. Cells were washed with PBS 3 times 3 h after infection. Subsequently viral RNA and 18S ribosomal RNA in the cells were quantified. All samples were analyzed in triplicate.

the molecules expressed after infection with its important role in viral replication [18–20], and the effect of nelfinavir on the main proteinase activity should be investigated. We have cloned, expressed, and purified SARS-CoV main proteinase in order to examine the effect of nelfinavir on this enzyme. Our preliminary study indicated that the activity of the main proteinase was blocked only partially (data not shown), which implies that nelfinavir may interact with some molecule(s) other than the main proteinase to fully inhibit SARS-CoV replication.

Nelfinavir is a very safe and widely used inhibitor of the HIV-1 protease, with strong in vivo activity in HIV-infected patients. Nelfinavir is generally used in combination with other antiretroviral medications as part of a highly active antiretroviral regimen (HAART) [21]. When used in this manner, 50–75% of patients who are naive to antiretroviral therapy have plasma HIV RNA levels below the limit of detection in association with an approximate increase of 200 mm^{-3} CD4(+) lymphocytes at 12 months of therapy [22–25]. The most common side effect of nelfinavir is mild diarrhea, which is observed in 15–20% of patients [26]. Nelfinavir is well tolerated by patients with HIV infection. Due to these characteristics, nelfinavir has become one of the most frequently prescribed first line protease inhibitors in the treatment of HIV-infected individuals.

Our studies have clearly shown that nelfinavir can strongly inhibit the replication of SARS-CoV in Vero E6 cells. The safety of this drug for humans has already been established, which constitutes the advantages of nelfinavir even for the clinical use to SARS patients. Our results suggest that nelfinavir should be examined clinically for the treatment of SARS. Moreover, nelfinavir might be a promising lead compound for anti-SARS drugs.

Acknowledgments

This work was supported by grants from the Ministry of Education, Science and Culture and the Ministry of Health, Labor and Welfare of Japan.

References

[1] N. Lee, D. Hui, A. Wu, P. Chan, P. Cameron, G.M. Joynt, A. Ahuja, M.Y. Yung, C.B. Leung, K.F. To, S.F. Lui, C.C. Szeto, S. Chung, J.J. Sung, A major outbreak of severe acute respiratory syndrome in Hong Kong, N. Engl. J. Med. 348 (2003) 1986–1994.

[2] S. M. Poutanen, D.E. Low, B. Henry, S. Finkelstein, D. Rose, K. Green, R. Tellier, R. Draker, D. Adachi, M. Ayers, A.K. Chan, D.M. Skowronski, I. Salit, A.E. Simor, A.S. Slutsky, P.W. Doyle, M. Krajden, M. Petric, R.C. Brunham, A.J. McGeer, C. National Microbiology Laboratory, T. Canadian Severe Acute Respiratory Syndrome Study, Identification of severe acute respiratory syndrome in Canada, N. Engl. J. Med. 348 (2003) 1995–2005.

[3] K.W. Tsang, P.L. Ho, G.C. Ooi, W.K. Yee, T. Wang, M. Chan-Yeung, W.K. Lam, W.H. Seto, L.Y. Yam, T.M. Cheung, P.C. Wong, B. Lam, M.S. Ip, J. Chan, K.Y. Yuen, K.N. Lai, A cluster of cases of severe acute respiratory syndrome in Hong Kong, N. Engl. J. Med. 348 (2003) 1977–1985.

[4] WHO, in, 2003.

[5] C.A. Donnelly, A.C. Ghani, G.M. Leung, A.J. Hedley, C. Fraser, S. Riley, L.J. Abu-Raddad, L.M. Ho, T.Q. Thach, P. Chau, K.P. Chan, T.H. Lam, L.Y. Tse, T. Tsang, S.H. Liu, J.H. Kong, E.M. Lau, N.M. Ferguson, R.M. Anderson, Epidemiological determinants of spread of causal agent of severe acute respiratory syndrome in Hong Kong, Lancet 361 (2003) 1761–1766.

[6] C. Drosten, S. Gunther, W. Preiser, S. van der Werf, H.R. Brodt, S. Becker, H. Rabenau, M. Panning, L. Kolesnikova, R.A. Fouchier, A. Berger, A.M. Burguiere, J. Cinatl, M. Eickmann, N. Escriou, K. Grywna, S. Kramme, J.C. Manuguerra, S. Muller, V. Rickerts, M. Sturmer, S. Vieth, H.D. Klenk, A.D. Osterhaus, H. Schmitz, H.W. Doerr, Identification of a novel coronavirus in patients with severe acute respiratory syndrome, N. Engl. J. Med. 348 (2003) 1967–1976.

[7] T.G. Ksiazek, D. Erdman, C.S. Goldsmith, S.R. Zaki, T. Peret, S. Emery, S. Tong, C. Urbani, J.A. Comer, W. Lim, P.E. Rollin, S.F. Dowell, A.E. Ling, C.D. Humphrey, W.J. Shieh, J. Guarner, C.D. Paddock, P. Rota, B. Fields, J. DeRisi, J.Y. Yang, N. Cox, J.M. Hughes, J.W. LeDuc, W.J. Bellini, L.J. Anderson, S.W. Group, A novel coronavirus associated with severe acute respiratory syndrome, N. Engl. J. Med. 348 (2003) 1953–1966.

[8] R.A. Fouchier, T. Kuiken, M. Schutten, G. van Amerongen, G.J. van Doornum, B.G. van den Hoogen, M. Peiris, W. Lim, K. Stohr, A.D. Osterhaus, Aetiology: Koch's postulates fulfilled for SARS virus, Nature 423 (2003) 240.

[9] W. Gao, A. Tamin, A. Soloff, L. D'Aiuto, E. Nwanegbo, P.D. Robbins, W.J. Bellini, S. Barratt-Boyes, A. Gambotto, Effects of a SARS-associated coronavirus vaccine in monkeys, Lancet 362 (2003) 1895–1896.

[10] L.K. So, A.C. Lau, L.Y. Yam, T.M. Cheung, E. Poon, R.W. Yung, K.Y. Yuen, Development of a standard treatment protocol for severe acute respiratory syndrome, Lancet 361 (2003) 1615–1617.

[11] K.L. Hon, C.W. Leung, W.T. Cheng, P.K. Chan, W.C. Chu, Y.W. Kwan, A.M. Li, N.C. Fong, P.C. Ng, M.C. Chiu, C.K. Li, J.S. Tam, T.F. Fok, Clinical presentations and outcome of severe acute respiratory syndrome in children, Lancet 361 (2003) 1701–1703.

[12] G. Zhaori, Antiviral treatment of SARS: can we draw any conclusions?, C.M.A.J. 169 (2003) 1165–1166.

[13] C.M. Booth, L.M. Matukas, G.A. Tomlinson, A.R. Rachlis, D.B. Rose, H.A. Dwosh, S.L. Walmsley, T. Mazzulli, M. Avendano, P. Derkach, I.E. Ephtimios, I. Kitai, B.D. Mederski, S.B. Shadowitz, W.L. Gold, L.A. Hawryluck, E. Rea, J.S. Chenkin, D.W. Cescon, S.M. Poutanen, A.S. Detsky, Clinical features and short-term outcomes of 144 patients with SARS in the greater Toronto area, Jama 289 (2003) 2801–2809.

[14] J. Cinatl, B. Morgenstern, G. Bauer, P. Chandra, H. Rabenau, H.W. Doerr, Treatment of SARS with human interferons, Lancet 362 (2003) 293–294.

[15] M.R. Loutfy, L.M. Blatt, K.A. Siminovitch, S. Ward, B. Wolff, H. Lho, D.H. Pham, H. Deif, E.A. LaMere, M. Chang, K.C. Kain, G.A. Farcas, P. Ferguson, M. Latchford, G. Levy, J.W. Dennis, E.K. Lai, E.N. Fish, Interferon alfacon-1 plus corticosteroids in severe acute respiratory syndrome: a preliminary study, Jama 290 (2003) 3222–3228.

[16] B.L. Haagmans, T. Kuiken, B.E. Martina, R.A. Fouchier, G.F. Rimmelzwaan, G. Van Amerongen, D. Van Riel, T. De Jong, S. Itamura, K.H. Chan, M. Tashiro, A.D. Osterhaus, Pegylated interferon-alpha protects type 1 pneumocytes against SARS coronavirus infection in macaques, Nat. Med. 10 (2004) 290–293.

[17] J. Cinatl, B. Morgenstern, G. Bauer, P. Chandra, H. Rabenau, H.W. Doerr, Glycyrrhizin, an active component of liquorice roots, and replication of SARS-associated coronavirus, Lancet 361 (2003) 2045–2046.

[18] V. Thiel, K.A. Ivanov, A. Putics, T. Hertzig, B. Schelle, S. Bayer, B. Weissbrich, E.J. Snijder, H. Rabenau, H.W. Doerr, A.E. Gorbalenya, J. Ziebuhr, Mechanisms and enzymes involved in SARS coronavirus genome expression, J. Gen. Virol. 84 (2003) 2305–2315.

[19] M.A. Marra, S.J. Jones, C.R. Astell, R.A. Holt, A. Brooks-Wilson, Y.S. Butterfield, J. Khattra, J.K. Asano, S.A. Barber, S.Y. Chan, A. Cloutier, S.M. Coughlin, D. Freeman, N. Girn, O.L. Griffith, S.R. Leach, M. Mayo, H. McDonald, S.B. Montgomery, P.K. Pandoh, A.S. Petrescu, A.G. Robertson, J.E. Schein, A. Siddiqui, D.E. Smailus, J.M. Stott, G.S. Yang, F. Plummer, A. Andonov, H. Artsob, N. Bastien, K. Bernard, T.F. Booth, D. Bowness, M. Czub, M. Drebot, L. Fernando, R. Flick, M. Garbutt, M. Gray, A. Grolla, S. Jones, H. Feldmann, A. Meyers, A. Kabani, Y. Li, S. Normand, U. Stroher, G.A. Tipples, S. Tyler, R. Vogrig, D. Ward, B. Watson, R.C. Brunham, M. Krajden, M. Petric, D.M. Skowronski, C. Upton, R.L. Roper, The genome sequence of the SARS-associated coronavirus, Science 300 (2003) 1399–1404.

[20] P.A. Rota, M.S. Oberste, S.S. Monroe, W.A. Nix, R. Campagnoli, J.P. Icenogle, S. Penaranda, B. Bankamp, K. Maher, M.H. Chen, S. Tong, A. Tamin, L. Lowe, M. Frace, J.L. DeRisi, Q. Chen, D. Wang, D.D. Erdman, T.C. Peret, C. Burns, T.G. Ksiazek, P.E. Rollin, A. Sanchez, S. Liffick, B. Holloway, J. Limor, K. McCaustland, M. Olsen-Rasmussen, R. Fouchier, S. Gunther, A.D. Osterhaus, C. Drosten, M.A. Pallansch, L.J. Anderson, W.J. Bellini, Characterization of a novel coronavirus associated with severe acute respiratory syndrome, Science 300 (2003) 1394–1399.

[21] J.S. Lewis 2nd, C.M. Terriff, D.R. Coulston, M.W. Garrison, Protease inhibitors: a therapeutic breakthrough for the treatment of patients with human immunodeficiency virus, Clin. Ther. 19 (1997) 187–214.

[22] G.P. Rizzardi, G. Tambussi, P.A. Bart, A.G. Chapuis, A. Lazzarin, G. Pantaleo, Virological and immunological responses to HAART in asymptomatic therapy-naive HIV-1-infected subjects according to CD4 cell count, Aids 14 (2000) 2257–2263.

[23] O. Kirk, J.D. Lundgren, C. Pedersen, L.R. Mathiesen, H. Nielsen, T.L. Katzenstein, N. Obel, J. Gerstoft, A randomized trial comparing initial HAART regimens of nelfinavir/nevirapine and ritonavir/saquinavir in combination with two nucleoside reverse transcriptase inhibitors, Antiviral Ther. 8 (2003) 595–602.

[24] R. Manfredi, L. Calza, F. Chiodo, Prospective comparison of first-line nelfinavir therapy versus nelfinavir introduction in rescue antiretroviral regimens, AIDS Patient Care Stud. 17 (2003) 105–114.

[25] S. Fleury, G.P. Rizzardi, A. Chapuis, G. Tambussi, C. Knabenhans, E. Simeoni, J.Y. Meuwly, J.M. Corpataux, A. Lazzarin, F. Miedema, G. Pantaleo, Long-term kinetics of T cell production in HIV-infected subjects treated with highly active antiretroviral therapy, Proc. Natl. Acad. Sci. USA 97 (2000) 5393–5398.

[26] S.W. Kaldor, V.J. Kalish, J.F. Davies 2nd, B.V. Shetty, J.E. Fritz, K. Appelt, J.A. Burgess, K.M. Campanale, N.Y. Chirgadze, D.K. Clawson, B.A. Dressman, S.D. Hatch, D.A. Khalil, M.B. Kosa, P.P. Lubbehusen, M.A. Muesing, A.K. Patick, S.H. Reich, K.S. Su, J.H. Tatlock, Viracept (nelfinavir mesylate, AG1343): a potent, orally bioavailable inhibitor of HIV-1 protease, J. Med. Chem. 40 (1997) 3979–3985.

Protease-mediated enhancement of severe acute respiratory syndrome coronavirus infection

Shutoku Matsuyama*, Makoto Ujike*, Shigeru Morikawa†, Masato Tashiro*, and Fumihiro Taguchi*‡

Division of Respiratory Viral Diseases and SARS, *Department of Virology III, Special Pathogens Laboratory, †Department of Virology I, National Institute of Infectious Diseases, Murayama Branch, Gakuen 4-7-1, Musashi-Murayama, Tokyo 208-0011, Japan

Edited by Peter Palese, Mount Sinai School of Medicine, New York, NY, and approved July 19, 2005 (received for review April 19, 2005)

A unique coronavirus severe acute respiratory syndrome-coronavirus (SARS-CoV) was revealed to be a causative agent of a life-threatening SARS. Although this virus grows in a variety of tissues that express its receptor, the mechanism of the severe respiratory illness caused by this virus is not well understood. Here, we report a possible mechanism for the extensive damage seen in the major target organs for this disease. A recent study of the cell entry mechanism of SARS-CoV reveals that it takes an endosomal pathway. We found that proteases such as trypsin and thermolysin enabled SARS-CoV adsorbed onto the cell surface to enter cells directly from that site. This finding shows that SARS-CoV has the potential to take two distinct pathways for cell entry, depending on the presence of proteases in the environment. Moreover, the protease-mediated entry facilitated a 100- to 1,000-fold higher efficient infection than did the endosomal pathway used in the absence of proteases. These results suggest that the proteases produced in the lungs by inflammatory cells are responsible for high multiplication of SARS-CoV, which results in severe lung tissue damage. Likewise, elastase, a major protease produced in the lungs during inflammation, also enhanced SARS-CoV infection in cultured cells.

cell entry | protease | spike protein | SARS

Severe acute respiratory syndrome (SARS) is caused by a SARS-associated coronavirus (SARS-CoV), a newly emergent member in a family of Coronaviridae (1–6). Unlike other human coronaviruses, SARS-CoV causes a fatal respiratory disease in humans (1–6). Coronavirus is an enveloped virus with a positive-stranded large genomic RNA with ≈30 kb (7). Spikes exist on the virion surface and resemble solar corona, each of which is composed of a trimer of the spike (S) protein (7, 8). The S protein is a type I fusion protein of an approximate molecular weight of 180 kDa. The prototypical coronavirus mouse hepatitis virus enters into cells via the cell surface, although a variant isolated from persistent infection enters from an endosome, the low pH of which induces its fusion activity (9). However, the entry pathway of SARS-CoV appears to be distinct from that of the other coronaviruses. Simmons *et al.* (10) hypothesized that SARS-CoV enters cells by an endosomal pathway, and S protein is activated for fusion by trypsin-like protease in an acidic environment. This idea is based on the following two findings: (*i*) SARS-CoV infection can be blocked by lysosomotropic agents, and (*ii*) S protein expressed on cells is activated for fusion by trypsin. These results were obtained by studies using pseudotype retroviruses harboring SARS-CoV S protein on the envelope and those using S protein expressed on cells by expression vectors (10).

In the present study, we show that various proteases, as well as trypsin, are effective in inducing the fusion of SARS-CoV-infected VeroE6 cells. These proteases facilitated SARS-CoV entry from the cell surface, which indicates that SARS-CoV has the potential to enter cells via two different pathways, either an endosomal or a nonendosomal pathway, depending on the presence of proteases. More interestingly, SARS-CoV entry from cell surface mediated by protease resulted in >100-fold more efficient infection than entry through endosome. Elastase, a major protease produced during lung inflammation, also manifested this enhancing effect. These findings suggest that severe illness in the lungs and intestines is attributable to the proteases produced in these organs during an inflammatory response or in the presence of certain physiological conditions.

Materials and Methods

Cells and Viruses. VeroE6 cells were grown in DMEM (Nissui, Tokyo), supplemented with 5% FBS (GIBCO/BRL). The SARS-CoV Frankfurt 1 strain, kindly provided by J. Ziebuhr (University of Würzburg, Würzburg, Germany) (1), was propagated and assayed by using Vero E6 cells.

Proteases. Various proteases were dissolved in PBS (pH 7.2) and used at the indicated concentrations in DMEM containing 5% FCS. The proteases used in this study were trypsin (Sigma, T-8802), thermolysin (Sigma, P 1512), chymotrypsin (Sigma, C-3142), dispase (Roche, 1 276 921), papain (Worthington, 53J6521), proteinase K (Wako, Tokyo), collagenase (Sigma, C-5183), and elastase (Sigma, E-0258).

Plaque Assay. VeroE6 cells prepared in 24-well plates were inoculated with 50 μl of 10-fold serially diluted virus samples and incubated at 37°C for 1 h. Cells were then cultured with 0.5 ml per well of DMEM containing 1% FCS and 0.75% methyl cellulose (Sigma) for 2 d. Cells were fixed with 1 ml of 10% formaldehyde per well for at least 2 h. After removing the culture fluids, cells were irradiated overnight under a UV lamp and stained with crystal violet. Plaques produced by SARS-CoV were counted under light microscopy. Titration was done in duplicate and infectivity was displayed by plaque-forming units (pfu).

Western Blotting. S protein expressed in Vero E6 cells was analyzed by Western blotting. Preparation of cell lysates, SDS/PAGE, and electrical transfer of the protein onto a transfer membrane were described (11). S protein was detected with anti-S Ab, IMG-557 (Imgenex, San Diego) and horseradish peroxidase-conjugated anti-rabbit IgG Ab (anti-R-IgG, ALI3404, BioSource International, Camarillo, CA). The bands were visualized by using enhanced chemiluminescence reagents (ECL-plus, Amersham Pharmacia) on a LAS-1000 instrument (Fuji).

Real-Time PCR. VeroE6 cells in 96-well culture plates were treated with DMEM containing 1 μM bafilomycin (Baf; Sigma, B-1793) and 5% FCS (DMEM plus Baf) at 37°C for 30 min and then chilled on ice for 10 min. Approximately 10^4 pfu of virus in DMEM plus Baf were infected to 10^4 cells on ice; multiplicity of

This paper was submitted directly (Track II) to the PNAS office.

Abbreviations: SARS-CoV, severe acute respiratory syndrome-coronavirus; S, spike; pfu, plaque-forming unit; moi, multiplicity of infection; Baf, bafilomycin.

‡To whom correspondence should be addressed. E-mail: ftaguchi@nih.go.jp.

© 2005 by The National Academy of Sciences of the USA

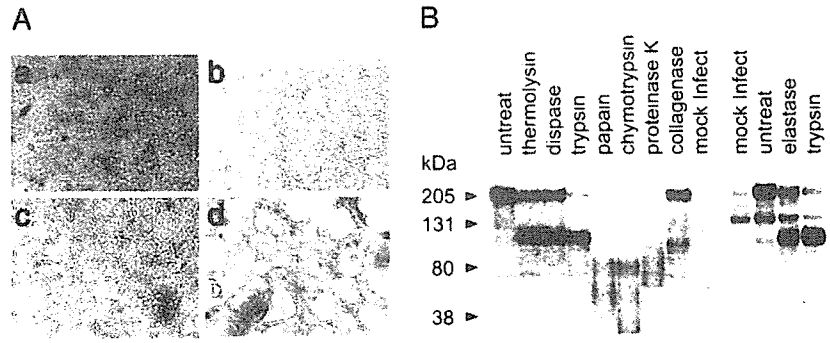

Fig. 1. Induction of cell-fusion and SARS-CoV S protein cleavage by proteases. (*A*) Syncytium formation after treatment with trypsin. VeroE6 cells cultured in 24-well plates were infected (*b* and *d*) or mock-infected (*a* and *c*) with the SARS-CoV Frankfurt 1 strain at moi = 0.5 and incubated at 37°C for 20 h. Cells were washed once with PBS and treated (*c* and *d*) or untreated (*a* and *b*) with 200 μg/ml trypsin for 5 min. Those cells were cultured for a further 4 h and observed by microscopy. (*B*) Western blot analysis of S protein treated with various proteases. Cells infected as described above were treated either with thermolysin (200 μg/ml), dispase (1 unit/ml), trypsin (200 μg/ml), papain (0.74 unit/ml), chymotrypsin (1 mg/ml), proteinase K (8 μg/ml) collagenase (200 μg/ml), or elastase (1 mg/ml), as described above. Soon after treatment, cells were lysed with lysing buffer, and S protein was analyzed by Western blot after SDS/PAGE. To detect the S protein (S2 fragment), mAb IMG-557 was used at a concentration of 5 μg/ml.

infection (moi) was at 1. After 30-min adsorption, the virus was removed, and infected cells were treated for 5 min with various concentrations of proteases in DMEM plus Baf that was prewarmed at room temperature. After protease was removed, cells were cultured in DMEM plus Baf at 37°C for 6 h. Vero E6 cell monolayers in 24-well plates were infected with 10 pfu of SARS-CoV (moi = 0.0001). After 30-min adsorption, cells were cultured in DMEM containing 5% FCS in the presence or in the absence of various proteases for 20 h. To isolate cellular RNA, 100 and 500 μl of isogen (Nippon Gene, Toyama, Japan) were added to each well of 96- and 24-well plates, respectively, together with 5 μg of yeast RNA as a carrier for 2-propanol precipitation. RNA was prepared according to the manufacturer's instructions and finally dissolved in 20 μl of diethyl pyrocarbonate-treated water. Real-time PCR was performed to estimate the amounts of mRNA9 in a final volume of 20 μl of 1× LightCycler RNA Master Mix (Roche Diagnostics) by using the RNA isolated as described above. For amplification of the fragment from mRNA9, we used 500 nM of a pair of oligonucleotides 5′-CTCGATCTCTTGTAGATCTG-3′ (SARS leader) and 5′-TCTAAGTTCCTCCTTGCCAT-3′ (SARS mRNA9 reverse). Amplified DNA from mRNA has 240 bases. With these primers, genomic RNA was not detected because the fragment to be amplified from genomic RNA would be ≈30 kb. For detection by hybridization, 200 nM each of the hybridization probes 5′-ACCAGAATGGAGGACGCAATGGGGCAAG-3′ (3′FITC labeled), 5′-CCAAAACAGCGCCGACCCCAAGGTTTAC-3′ (5′LCRed640 labeled) were used. PCR analysis was performed under the following conditions [reverse transcription: 61°C, 20 min; PCR, 95°C, 30 s (95°C, 5 s; 55°C, 15 s; 72°C, 10 s) ×45 cycles] with a LightCycler instrument (Roche Diagnostics). To measure the amounts of viruses that entered into cells, we infected cells with 10-fold stepwise diluted SARS-CoV from 10^6 to 10^2 pfu, and the amounts of mRNA9 were determined by real-time PCR. The amounts of virus that entered into cells after protease treatment were calculated from a calibration line obtained as above and shown as relative mRNA levels. When relative mRNA9 was higher than 10^6 pfu, samples were diluted and reexamined so that they were placed between 10^6 and 10^2 pfu.

Results

Activation of Cell Fusion and SARS-CoV S Protein Cleavage by Various Proteases. VeroE6 cells susceptible to SARS-CoV were infected with the Frankfurt-1 strain of SARS-CoV at a moi of 0.5, and those infected cells were treated with trypsin at 20 h after infection. Cell fusion was detected from 2 h after trypsin treatment (Fig. 1*Ad*). Fusion was also found after treatment with thermolysin or dispase (data not shown). Little or no fusion occurred after treatment with papain, chymotrypsin, proteinase K, or collagenase. S proteins in cells treated with proteases that induce fusion were cleaved approximately in the middle (Fig. 1*B*), a finding similar to that of Simmons *et al.* (10). In contrast, no apparent S2 band was detected in cells bearing S proteins treated with proteases that failed to induce fusion (Fig. 1*B*). These results showed that various proteases, including trypsin, activate the fusion activity of the SARS-CoV S protein by inducing its cleavage. Further, SARS-CoV infection was extensively inhibited by treatment of cells with Baf (Fig. 2*A*, no Baf vs. Baf without protease). These results suggest that SARS-CoV takes an endosomal pathway for its entry, and that S protein cleavage is important for fusogenicity, which is consistent with the conclusions of a previous report (10).

SARS-CoV Entry from Cell Surface Facilitated by Proteases. If the hypothesis proposed by Simmons *et al.* (10) is correct, we can make SARS-CoV enter cells directly from their surface by attaching the virus there and treating them with trypsin and other proteases that induce fusion. Treatment of VeroE6 cells with Baf at a concentration of 1 μM suppressed SARS-CoV infection via the endosomal pathway to <1/100, as shown in Fig. 2*A*. The cells treated with Baf were inoculated with SARS-CoV at a moi of 1 and incubated on ice for 30 min (adsorption on ice does not allow virus to enter cells). Then cells were treated with various proteases for 5 min at room temperature and incubated at 37°C for 6 h. Virus entry was estimated by the newly synthesized mRNA9 measured quantitatively by real-time PCR. A calibration curve of real-time PCR (Fig. 2*C*), showing the level of mRNA9 after infection with 10-fold diluted SARS-CoV, was used to estimate the amount of infected virus from the mRNA levels. As shown in Fig. 2*A*, thermolysin and trypsin, two proteases with fusion-inducing activity, extensively facilitated viral entry. In contrast, two proteases that did not induce fusion, papain and collagenase failed to do so. Treatment of cells with trypsin before virus infection did not facilitate viral entry (Fig. 2*B*), indicating that effects of trypsin on cells are not involved in this infection. Other proteases did not influence the SARS-CoV infection as trypsin, when treated before virus inoculation (data not shown). Protease treatment of SARS-CoV before infection did not enhance infectivity but reduced it by 10- to 100-fold (data

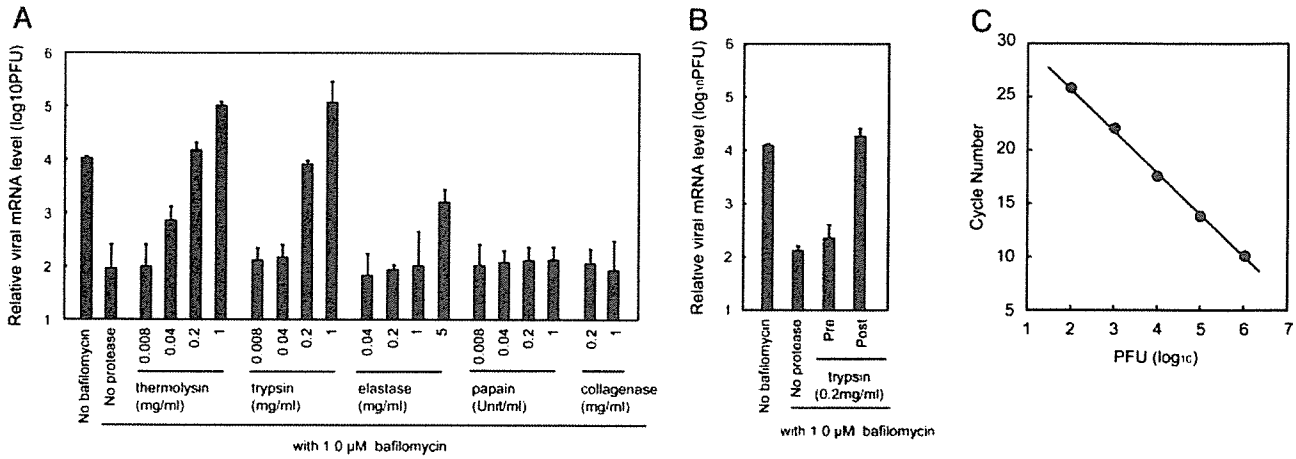

Fig. 2. Entry of SARS-CoV from cell surface facilitated by proteases. (*A*) Effect of proteases on SARS-CoV entry into VeroE6 cells treated with Baf. VeroE6 cells in 96-well plates were treated with Baf at a concentration of 1 μM at 37°C for 30 min, placed on ice and infected with SARS-CoV at moi = 1 for 30 min. Then, cells were treated with various concentrations of different proteases at room temperature for 5 min and cultured in the presence of Baf for a further 6 h. The amount of mRNA9 was measured quantitatively by real-time PCR. Cells untreated with Baf or those treated with Baf but untreated with protease were used as controls. The relative viral mRNA level is displayed by virus infectivity (pfu) calculated from a calibration line shown in *C*. (*B*) Cells treated with Baf at 37°C for 30 min were then treated with trypsin at room temperature for 5 min before (pre) or after (post) virus inoculation, and virus infection was estimated quantitatively by real-time PCR as described above. (*C*) Calibration in real-time PCR. VeroE6 cells in 94-well plates were infected with 10-fold step diluted viruses, and mRNA9 levels at 6 h after infection were estimated by real-time PCR. The relationship is shown between inoculated pfu (*x* axis) and cycles of real-time PCR to reach a positive level (amount of mRNA9) (*y* axis).

not shown). We believe these results demonstrate that SARS-CoV, when adsorbed onto the cell surface, fuse with the plasma membrane of its envelope with S protein, which is cleaved into S1 and S2 by proteases with fusion-inducing activity. This suggests a nonendosomal, direct entry of SARS-CoV into cells in the presence of proteases. Those findings also support the hypothesis drawn by Simmons *et al.* (10) that trypsin-like protease plays an important role in facilitating membrane fusion.

Enhancement of SARS-CoV Infection by Various Proteases. Treatment with a high concentration of thermolysin and trypsin augmented virus entry or replication by 10-fold or higher, as compared with the standard infection (Fig. 2*A*, e.g., compare bar 6 or bar 10 with bar 1 from the left). We then compared the replication kinetics of SARS-CoV in cells treated with Baf and a high concentration of trypsin with that of cells maintained without Baf or trypsin. The level of mRNA9 was always ≈10-fold higher in trypsin-treated cells at any given time during the early period of infection (Fig. 3). These data also imply that viral replication after entry via the cell surface proceeds ≈1 h ahead of that via the endosomal pathway, suggesting that the surface route is more efficient for rapid viral replication.

Because SARS-CoV replication was shown to be enhanced by trypsin treatment, we next assessed the efficiency of virus spread in the presence or absence of trypsin in a low moi, which mimics natural infection in target organs. Virus (10 pfu) were inoculated onto 10^5 confluent VeroE6 cells (moi = 0.0001), and the cells were incubated at 37°C for 20 h in the media with or without trypsin. The level of mRNA9 estimated quantitatively by real-time RT-PCR showed that virus replication was 100- to 1,000-fold higher when cells were cultured in the presence of trypsin, when compared with replication in the absence of trypsin (Fig. 4*A*). Viral infectivity of the supernatants in SARS-CoV-infected cells cultured with or without trypsin also indicated that trypsin treatment enhanced viral growth by ≈100-fold (Fig. 4*B*). We also examined growth kinetics of SARS-CoV in the presence of low-concentration proteases (62.5 μg/ml trypsin, 125 μg/ml elastase) that do not detach cells from plates during culture for 42 h. It was also shown that protease enhanced virus replication (Fig. 4*C*) with remarkable fusion formation (Fig. 4*D*). All of these results strongly suggest that the virus spreads efficiently from cell to cell in the presence of trypsin, which cleaves S to S1 and S2 to allow cell entry of SARS-CoV via the cell surface.

We next examined the effects on low moi by other proteases that facilitate SARS-CoV entry from VeroE6 cell surface. As shown in Fig. 5, all of the proteases that produce S2 (Fig. 1*B*) and that induce cell-cell fusion enhanced virus spread. In contrast, those proteases that did not generate S2 and that did not induce cell-cell fusion failed to enhance the infection. These observations suggest that proteases that facilitate SARS-CoV entry from the cell surface support efficient SARS-CoV infection. Thus, protease is likely to be responsible for the high multiplication of

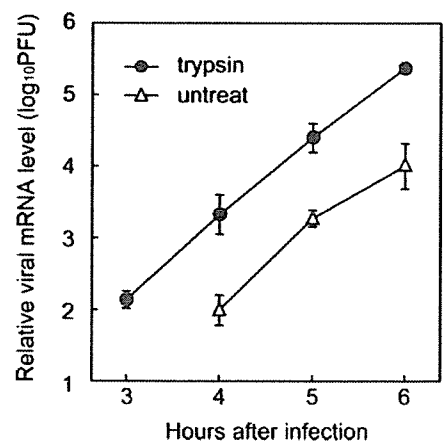

Fig. 3. Kinetics of mRNA9 synthesis after treatment of trypsin. VeroE6 cells were treated with Baf, infected with SARS-CoV, and treated with 200 μg/ml trypsin as described in the legend to Fig. 2*A*. The amount of mRNA9 synthesized was monitored by real-time PCR at 3–6 h after inoculation. VeroE6 cells without any treatment were also infected as a control (untreated). Relative viral mRNA level is displayed by virus infectivity (pfu) calculated from the calibration line shown in Fig. 2*C*.

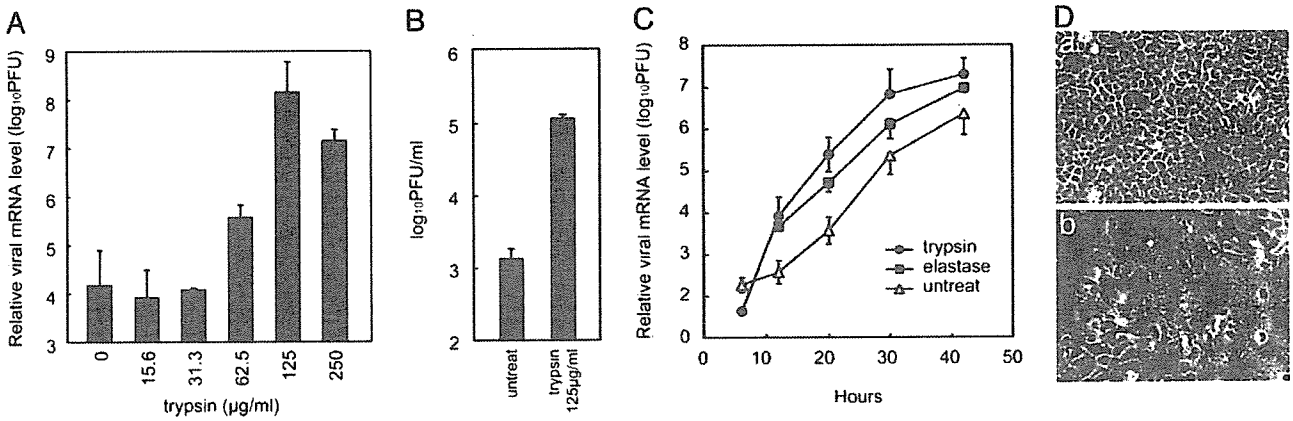

Fig. 4. Enhancement of SARS-CoV infection by proteases. (*A*) Effect of trypsin on virus replication in VeroE6 cells. Approximately 1×10^5 VeroE6 cells cultured in 24-well plates were infected with 10 pfu of SARS-CoV (moi = 0.0001) and cultured in the presence of varied trypsin concentrations. Viral replication was estimated at 20 h after infection by the amount of mRNA9, as measured by real-time PCR. (*B*) Viral infectivity was examined by plaque assay after 20-h incubation in the presence or absence of trypsin (125 μg/ml). (*C*) Viral growth kinetics after infection was examined in cultures in the presence or absence of trypsin (62.5 μg/ml) or elastase (125 μg/ml) by real-time PCR. Cells were harvested from 4 to 42 h after infection at intervals and the level of mRNA9 was monitored. Relative viral mRNA level is displayed by virus infectivity (pfu) calculated from a calibration line (*A–C*). (*D*) Cytopathic changes of virus-infected cells cultured in the presence (*b*) or absence (*a*) of trypsin (125 μg/ml) for 42 h are shown.

SARS-CoV in the major target organs of SARS, such as the lungs and bronchus, where various proteases are produced (e.g., by inflammatory cells), as well as in the intestines, where a number of proteases are physiologically secreted.

One of the major proteases produced by inflammatory cells in the lungs is an elastase produced by neutrophils (12), the accumulation of which was reported in the lungs of SARS patients (13). The level of elastase in bronchoalveolar lavage fluids was reported to reach levels as high as 700 μg/ml (12). Accordingly, we determined whether this protease has the potential to enhance SARS-CoV infection in a fashion similar to that of trypsin or thermolysin. Elastase was revealed to enhance SARS-CoV infection in cultured VeroE6 cells in terms of S protein cleavage (Fig. 1*B*), its cell-surface-mediated entry pathway (Fig. 2*A*), and its growth enhancement ability after low moi (Figs. 4*C* and 5). These results strongly suggest that SARS-CoV replication can be enhanced in the lungs by elastase.

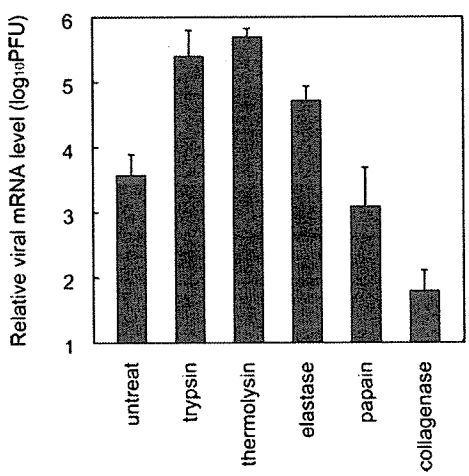

Fig. 5. Effect of various proteases on virus replication in VeroE6 cells. VeroE6 cells in 24-well plates were infected as described in Fig. 4 and cultured in the presence of trypsin (62.5 μg/ml), thermolysin (12.5 μg/ml), elastase (125 μg/ml), papain (0.037 unit/ml), or collagenase (200 μg/ml). At 20 h after infection, the amounts of mRNA9 were measured by real-time PCR. Relative viral mRNA level is displayed by virus infectivity (pfu) calculated from the calibration line.

Discussion

The SARS-CoV gene and viral antigens were found in a number of organs, such as the liver, cerebrum, pancreas, and kidneys, as well as in such major target organs as the bronchus, lungs, and intestines (14–17), with the latter showing drastic tissue damage by SARS-CoV infection, whereas the other organs were not so severely affected. Although the pathogenic mechanism of SARS has not been elucidated, the present study suggests that proteases secreted in major target organs play an important role in the high multiplication of virus in those organs, which, in turn, results in severe tissue damage. An initial infection by SARS-CoV in pneumocytes via its receptor ACE2 (18), the endosomal pathway, could induce inflammation that generates a variety of proteases such as elastase. Once those proteases are present in the lungs, they may mediate an ensuing robust infection, which may result in enhanced replication of SARS-CoV in the lungs. Although lung damage is postulated to be mediated by cytokines by a so-called cytokine storm (14, 16), higher virus multiplication could also contribute to the cytokine storm by killing a large number of infected cells. A variety of proteases secreted in the small intestines, another major target organ of SARS-CoV, could also be responsible for the high growth of SARS-CoV in these tissues, which could result in a high rate of diarrhea in SARS patients (19, 20).

Protease-mediated enhancement of infection is known for orthomyxovirus and paramyxovirus infections (21–24), in which their envelope glycoprotein is not fully cleaved in *de novo* synthesized cells, and thus the virus particles produced contain partially cleaved or uncleaved glycoprotein. Those glycoproteins on virions are cleaved after treatment with protease, which results in the enhancement of infectivity. Thus, trypsin affects directly virons and increases the infectivity of those viruses. However, enhancement of SARS-CoV infection by trypsin or other proteases is mediated by another mechanism. Although trypsin treatment *in vitro* induces cleavage of the S protein on virions, such treatment never enhances SARS-CoV infectivity but reduces it to 1/10–1/100 of the original titer. Only S protein bound to its receptor ACE2 and cleaved by proteases could obtain fusion activity. Based on this idea, it is most likely that